University of Minnesota
ST. ANTHONY FALLS HYDRAULIC LABORATORY

Project Report No. 139

CERRON GRANDE PROJECT

by
Charles C. S. Song

Conducted for the
COMISION EJECUTIVA HIDROELECTRICA DEL RIO LEMPA
El Salvador, Central America
and the
HARZA ENGINEERING COMPANY

January 1973
Minneapolis, Minnesota

CONTENTS

PREFACE

The model test described in this report was sponsored by the Harza Engineering Company of Chicago, Illinois, and the Hydroelectric Power Commission of the Lempa River, El Salvador, Central America. The model was constructed during the period between June and September of 1972. The model test was started immediately after the construction and completed in January of 1973. A brief and unedited motion picture showing the major components of the model and several views of the testing was also made.

The experiments were performed at the St. Anthony Falls Hydraulic Laboratory under the general direction of Edward Silberman and the immediate supervision of Charles C. S. Song. The models were fabricated in the laboratory shops, with much of the research carried on by Chyisheng Hwang, Earl C. Bancroft, and Zvi Krischer.

SUMMARY

This report describes the results of a hydraulic model test for the Cerron Grande hydroelectric power project. A 1:100 undistorted scale model including the spillway, the power intake and outlet, the headwater approach channel, the spillway exit channel, and a portion of the existing river downstream of the proposed dam site was constructed and tested. All major features of the model performed satisfactorily. The deflector at the downstream end of the spillway was very effective and operated satisfactorily over the entire range of discharges tested. Concentrated vortices were found at the spillway gates when the four gates were not open equally.

Commercial sand of 0.6 mm mean size was used for the downstream bed material everywhere except in the spillway exit channel immediately downstream of the spillway. For most experimental runs, erodible material in the form of 6 mm gravel was used as the bed material in the spillway exit channel. For this condition the impact force of the spillway jets produced a large scour hole in the exit channel and deposited the material immediately downstream. Otherwise, very little sediment movement was observed. Some experiments were also conducted after the exit channel was made nonerodible using concrete. For this condition the energy of the spillway flow was largely undissipated before the flow left the exit channel, and this caused a large amount of sediment movement in the tailrace.

CERRON GRANDE PROJECT

I. INTRODUCTION

The Cerron Grande Project is a hydroelectric power project being designed for the Hydroelectric Power Commission of the Lempa River, El Salvador, C.A. Harza Engineering Company International serves as the consulting engineer for the project. The Cerron Grande damsite is located at the headwater of the 5 de Noviembre reservoir, about 22 kilometers upstream of the existing dam. At the selected reservoir level, elevation 243 meters, the project will develop a maximum gross head of about 62 meters for power generation. A rock-and-sand-fill dam with an impervious clay core is to be built to elevation 250. A concrete chute spillway is provided on the left bank for a discharge capacity of about 10,000 cubic meters per second at the maximum headwater elevation of 250.0. The powerhouse intake structure is located on the right bank of the approach channel just upstream of the spillway gate structure. Immediately downstream of the spillway is an exit channel leading to the river. Two power generating units with a combined design discharge of 270 cms will be installed initially, but provisions will be made for adding two more identical units at a later date.

Since a large amount of fine sediment has been deposited in the river channel due to the existing reservoir downstream, and since the channel downstream of the spillway is erodible, there is concern about possible silting at the powerhouse exits and increased tailwater elevation due to delta formation. There is also concern over possible interference of the spillway flow with the power intake flow and the hydraulic performance of the spillway. A model study was conducted at the St. Anthony Falls Hydraulic Laboratory to determine the hydraulic performance of the proposed structures and the erosion pattern to be expected after the construction of the dam. A 1:100 scale undistorted model was constructed and tested. The results of the model tests are summarized in this report.

II. GENERAL DESCRIPTION OF THE MODEL

The main features of the 1:100 scale undistorted model are a headbox, a spillway, a power intake and outlet, and the erodible riverbed. The topography and the dimensions of the structures were modeled according to drawings

D. Erodible Bed

According to information supplied by the Harza Engineering Company*, the riverbed consists of a thick layer of sand overlying scattered lenses of sand and gravel. The sand in the river near the site is fine- to medium-grained, averaging approximately 90 per cent finer than No. 4 and less than 5 per cent finer than No. 200. At the downstream end of the dam site there are deposits of even finer material due to the delta formation which resulted from the construction of the existing downstream dam. For this reason, a considerable amount of sediment movement can be expected in the event of a flood after the dam and spillway have been constructed. Since the prototype riverbed material is sand, precise modeling of grain size was impractical. Therefore a commercially available sand of 0.6 mm mean size was used as the bed material in the model. The results of a sieve analysis of this material are shown in Fig. 5.

The exit channel downstream of the spillway will be excavated in agglomerate and tuff breccia, which are usually well cemented and strong rocks. However, their resistance to the impact of the high-velocity spillway flow is not known. For this reason, Harza Engineering Company specified two different types of materials to be used to simulate the exit channel. For most of the experiments, nearly uniform 6 mm diameter gravel having the size distribution indicated in Fig. 6 was used as the bed material for the exit channel. The gravel was placed between two sheet metal walls which extended from the floor of the model, El. 150.0, to El. 178.0. Some experiments were also carried out in the model using a non-erodible exit channel wherein the gravel bed had been replaced by a concrete floor at El. 178. As will be discussed later, the actual flow conditions in the prototype will depend very much on the erodibility of the rock foundation and the sequence of flood occurrence.

E. Tailgate and Downstream Conditions

The downstream end of the model riverbed terminated with a template serving as a wall. This template effectively fixed the bed profile at this cross section, and any sediment moving past it was trapped in the one-meter-

*Cerron Grande Project, A Feasibility Study, by Harza Engineering Company International in association with Atilio Garcia Prieto y Compania, March 1972.

wide sand trap. A hydraulically operated gate located at the downstream end of the sand trap was used to control the tailwater elevation according to the rating curve furnished by Harza Engineering Company.

III. EXPERIMENTAL RESULTS

A. Headwater-Discharge Rating Curves

At the beginning of the model test all the orifice meters in the intake pipes were calibrated using the hydraulic laboratory weighing tank. The probable error of the flow calibration is believed to be less than 5 per cent. Since some question was raised later about the validity of the calibration, the calibration curve was also calculated from the standard orifice formula. Results are discussed in the Appendix.

Since the headwater-discharge rating curve is independent of the erosion patterns downstream of the spillway, this series of tests was conducted first without sand or gravel in the model. The test was carried out for various gate opening combinations: all gates fully open, four gates in uniform partial positions, and individual gates operating in various positions from fully closed to fully open. For a fixed gate opening condition, various amounts of discharge, increasing in steps from zero to the maximum, were run through the model. The resulting headwater elevations at equilibrium conditions were measured with a point gage located 300 m upstream of the spillway. In order to find the interference effect of the power intake on the spillway flow rating curve, experiments were carried out with and without power intake flow. The results for cases in which four gates are equally open are plotted in Fig. 7. As can be seen from Fig. 7, powerhouse intake flow has a negligible effect on the headwater-discharge rating curve. Similar results for single gate operation are plotted in Fig. 8. The effect of powerhouse intake flow on the rating curve is again very small except at extremely small discharges. The rating curves for single gate operations were found to be almost identical for all four gates. For these reasons, rating curves relating the headwater elevation and the spillway discharge can be constructed using the data shown in Figs. 7 and 8.

A family of headwater-discharge rating curves constructed for several gate openings is shown in Figs. 9 and 10. These rating curves were obtained by interpolation using the data shown in Figs. 7 and 8 and taking into account the influence of the powerhouse intake flow where necessary.

B. Approach Flow Conditions

The approach flow patterns were observed for various discharges and gate opening conditions. Photos 3 through 6 show the flow patterns on the water surface made visible by confetti traces. These photographs are arranged in a sequence of increasing discharges, all with uniform gate openings and a powerhouse intake flow of 270 cms. Clearly, in all cases flow separation occurred and eddies formed in front of the powerhouse intake due to the sharp corner in the approach channel. The intensity of the separation eddy increased as the discharge increased. These eddies appear to have been little affected by the powerhouse intake flow and to be strictly products of the flow separation at the sharp corner. No measurements were taken to determine the intensity of the vortex in the flow through the powerhouse intake structure. However, the vortex appears to be localized near the water surface and to have little influence on the flow through the intake structure.

Frequently, vortices were observed at the spillway gates when not all gates were equally open. A pair of vortices occurred when one gate was partially open and the rest were closed. The vortex pairs are exemplified by Photo 7, which was taken for $Q = 850$ cms with one gate about half open. As the spillway discharge increased, the vortices in front of the spillway gate became unstable and intermittent. Since these vortices were transient in nature and often sucked air through the core, it seems likely that similar vortices appearing in the prototype would produce large transient forces on the gate. Although no systematic study has been carried out, it appears likely that the vortices were caused by boundary layer flow separation near the nose of the pier when the flow approached the pier at an angle. This induced angle of attack was the result of the lateral flow from the dead water zone to the opening. In fact, when two neighboring gates were not open equally, a vortex was almost always observed on the side of the pier where the gate opening was greater. This phenomenon is similar to that of an air foil stall when the angle of attack is excessively large. It is therefore recommended that the gate openings be kept as uniform as possible at all times to avoid vibratory forces due to vortex formation.

The effect of the hill upstream of the approach channel on the approach flow pattern was studied by observing the flow first without the hill and then with it. Only a very minor difference was noticeable, and there appears to be no hydraulic reason to remove this hill.

C. Flow Conditions in the Spillway

Water surface profiles on the centerline of each bay and along each side of the partition walls of the spillway were measured for various discharges using a point gage. There were no significant differences among the water surface profiles on the centerlines of the various bays, although the flow in the bay closest to the powerhouse was found to be somewhat more unsteady than the flows in the other bays. Measured water surface profiles on the centerlines at the normal maximum discharge of 5700 cms and those at the maximum discharge of 10,000 cms are shown in Figs. 11 and 12, respectively. Clearly, the differences between bays are very small and can be considered negligible. The average water surface profiles along the centerlines of all four bays for four different discharges are plotted in Fig. 13 for comparison. All the water surface profiles along the partition walls are very close to each other except those in Bay 1 (the bay closest to the powerhouse). Figure 14 shows the average water surface profile of all bays along the walls and the profiles along the right and left walls of Bay 1 for normal maximum discharge.

The mean pressure distribution on the ogee and along the centerline of the spillway surface as measured with static pressure taps is plotted in Fig. 15. The pressure distribution on the walls and off the centerline of the spillway surface is shown in Fig. 16. No negative pressure was observed under any of the flow conditions tested. Pressure fluctuations were also measured at the two locations shown in Fig. 4 using pressure transducers which have good frequency response up to 300 Hz. Sample pressure records are shown in Fig. 17. These measurements indicated that a major portion of the fluctuation energy was in a relatively high frequency range in the neighborhood of 100 Hz. Moreover, the amplitude of the fluctuations appeared to be very small, approximately 10 per cent of the static pressure head.

The selected deflector was effective in producing jets for all flow conditions tested. This type of deflector was necessitated by the low head, about 50 meters. Sweepout of low flows from a conventional flip bucket would have been a problem. Therefore, the wedges were included to concentrate the flow for low discharges, when sweepout is a problem, but allow the full width of the bucket for higher flows. We believe the resulting flip trajectory at low flows (< 3000 cms) is very good, while at higher flows the trajectory may be short of the desirable range. For discharges equal to 1000 and 3000 cms, individually identifiable jets sprung from each bay.

For flows equal to or greater than 5700 cms the jets spread laterally and it became difficult to identify the individual jets. The impact point of the jet measured from the lip was 67 m at $Q = 1000$ cms, increased to 87 m at $Q = 3000$ cms, and then decreased to 70 m at $Q = 5700$ cms.

D. Downstream Flow and Scour Pattern

Since the flow conditions downstream of the spillway and near the powerhouse were closely related to the scour pattern in that area, it is appropriate to discuss the two subjects simultaneously. The scour pattern, and hence the flow, was found to be very sensitive to the type of material used as bed material in the exit channel. At the request of Harza Engineering Company, only two types of materials (6.0 mm gravel and non-erodible concrete floor) were tested. The purpose of using the two materials in the exit channel was to bracket the prototype conditions. The erodible gravel would simulate a highly erodible material which breaks up into relatively small, uniform pieces. The rigid bed would simulate a very resistant material which does not permit a plunge pool to develop in the exit channel. It was hoped that from the results with these two extreme conditions, a judgment could be made as to the effects of any condition between the two extremes.

1. Test Results with 6.0 mm Gravel in Exit Channel

Prior to the experiments, the topography of the area immediately after construction as furnished by Harza Engineering Company was reproduced to scale as shown in Fig. 18. In the exit channel 6.0 mm gravel was used as bed material from El. 178.0 to El. 150.0; 0.6 mm sand was used in the remainder of the model. A series of three 90-minute runs was carried out with total discharges equal to 1000 cms, 3000 cms, and 5700 cms, respectively. The powerhouse flow was kept at 270 cms for all runs. At the end of each 90-minute run the flow was stopped and the erosion pattern recorded. The bed profile was not restored to the original condition before the next run was started. Thus the topographic maps shown in Figs. 19, 20, and 21 indicate the cumulative effect of consecutive floods of successively increasing magnitude. It appeared that the 90-minute model running time was sufficient for the erosion pattern to stabilize, at least in the immediate neighborhood of the exit channel. According to Froude law, 90 minutes of model time are equivalent to 15 hours of prototype time.

The most significant characteristic of this sequence of runs is the very rapid scouring of the gravel in the exit channel and the resulting deposition of gravel at the junction with the river to form a delta. The surface elevation of this delta was approximately 187 meters, and its area increased with the discharge. The periphery of the delta is indicated by a dotted curve in Figs. 19, 20, and 21. The scouring of the exit channel and the subsequent formation of the delta are shown for various flow rates in Photos 8, 9, and 10. It should be noted that the gravel delta was very effective in preventing scouring of the sand bed in its neighborhood. This delta not only served as a protective blanket, but also caused the flow to spread laterally, thus reducing the velocity of the flow.

In order to determine the effect of previous smaller floods on the scouring pattern due to a larger flood, the model was run at $Q = 5700$ cms for 90 minutes starting from an original topographic condition. The resulting erosion pattern is shown in Photo 11 and a topographic map in Fig. 22. Comparison of this figure with Fig. 21 reveals that the gravel delta is more widely spread in Fig. 22, but its average surface elevation is approximately 3 meters lower than that in the previous case. Consequently, there appears to have been more deposition in the area immediately downstream of the delta when the 5700 cms had not been preceded by lesser floods. Both Fig. 21 and Fig. 22 indicate a tendency for the sand to be carried upstream and deposited there by eddy currents. This upstream movement of the sand was very limited and in no case affected the powerhouse. Photo 12, showing a view of the powerhouse exit after the run with $Q = 5700$ cms, clearly illustrates this point. The wave height at the powerhouse was found to be less than one meter, and therefore no wave record was taken.

2. Test Results with Non-Erodible Exit Channel

The final run was made with a solidified exit channel at a discharge of 5700 cms. The results were drastically different from those of all the previous runs with the erodible exit channel. Since there was no erosion of the exit channel or subsequent deposition to form a protective delta, there was severe scouring in the river channel downstream of the concrete bed due to the high velocity jet. In contrast to the other cases, there was very little lateral spreading of the jet, and its energy did not dissipate until far downstream. Photo 13 shows the flow looking downstream. Accompanying

this high-momentum jet is a pair of strong vortices, one to the right, rotating clockwise, and the other to the left, rotating counterclockwise. Photos 14 and 15 show the pattern and give a rough idea of the intensity of these vortices.

As was mentioned before, the jet issuing from the concrete exit channel was so intensive that it scoured large quantities of sand and formed a deep trench; this can be seen in Photo 16. This photo, taken looking upstream, also shows severe scouring of the left embankment due to the high-intensity vortex. The velocity of this vortex near the embankment was measured as approximately 3 meters per second in prototype. This erosion of the left bank should be less severe in the prototype, since it is a fairly resistant rock similar to the exit channel. Some of the eroded sand was washed downstream, but much of it was carried upstream toward the powerhouse by the vortex to the right of the mainstream. This upstream movement of the sand took the form of a moving sandbar, as shown in Photo 17. This photograph was taken after 90 minutes of flow time at a discharge of 5700 cms. Although the movement of the sandbar was quite rapid during the first few minutes of flow, it had practically ceased to move upstream by the end of the 90 minute period. As can be noted from the photograph, the sandbar stopped moving short of the powerhouse. The erosion pattern after 90 minutes of flow is shown in Fig. 23 and the change after 90 more minutes of run time in Fig. 24. Very little change is noticeable between these two figures.

The scour pattern and the movement of the sandbar as described above should be taken only as qualitative indicators of what might happen in the prototype. Since the sediment was not selected according to the scale ratio, and since oversized sand was used in this model test, greater sediment movement can be expected in the prototype. For this reason it is possible that some sediment will be carried to the powerhouse from downstream, particularly if the exit channel is very resistant to erosion.

Before this experiment was concluded, the model was run at the maximum discharge of 10,000 cms. The model was capable of passing a flow of this magnitude without the dam being overtopped; at a few locations the internal spillway walls were overtopped. The headwater elevation was 249 m. Naturally, there was considerable sediment movement in the river, but no detailed observation was made.

Table 1. SUMMARY OF FLOW DATA

Total Discharge cms	Power Discharge cms	Exit Channel Condition	Headwater Elevation m	Tailwater Elevation m	Powerhouse Water Elev. m	Distance to Impact Point m
540	540	6.0 mm gravel	---	184.3	185.6	--
1,000	270	" " "	243	185.7	187.3	67
3,000	270	" " "	243	187.9	188.7	87
5,700	270	" " "	243	190.2	191.2	70
10,000	0	" " "	249	192	---	--
5,700	270	Concrete surface	243	190.2	189.0	70

IV. CONCLUSIONS

A 1:100 scale model of the Cerron Grande Project representing the spillway, powerhouse, and related structures was constructed and tested. The hydraulic performance of the structures for flood flows ranging from 540 cms to 10,000 cms--with emphasis on 1000 cms, 3000 cms, and 5700 cms--was studied. The performance of hydraulic features such as the approach channel, the spillway, and the deflectors was found to be satisfactory. Sediment erosion and deposition patterns downstream of the spillway and powerhouse were also studied. The results varied greatly depending upon the erodibility of the spillway exit channel. When the bed material in the exit channel was readily erodible, the impinging jet produced a large scour hole in the channel and deposited the eroded material immediately downstream of the exit channel to form a delta. As a result, the energy of the impinging jet was largely dissipated within the exit channel and the flow was spread rather uniformly in the lateral direction over the delta. Due to the greatly reduced velocity of the flow and the protective effect of the delta, there was very little scouring in the river. In fact, there were small deposits in various places.

On the contrary, when the exit channel was non-erodible, there was very little energy dissipation in the exit channel, and a jet of large momentum issued from the channel. This high-velocity flow resulted in deep scouring

in the river downstream of the exit channel and substantial erosion of the left embankment. A large amount of eroded sediment was carried upstream toward the powerhouse by strong vortex motion. Under the laboratory conditions, this upstream movement of the sediment took the form of a moving sandbar which stopped short of the powerhouse.

Since the model test did not reproduce the geological conditions in the spillway exit channel or represent the sediment according to the law of dynamic similarity, the actual erosion pattern and sediment movement which will occur in the prototype may be considerably different from that in the model. An additional complication in predicting prototype performance is uncertainty concerning the magnitude and sequence of actual flood discharges. The sediment movement due to a particular flood discharge will very likely be influenced by the conditions which precede it.

LIST OF FIGURES

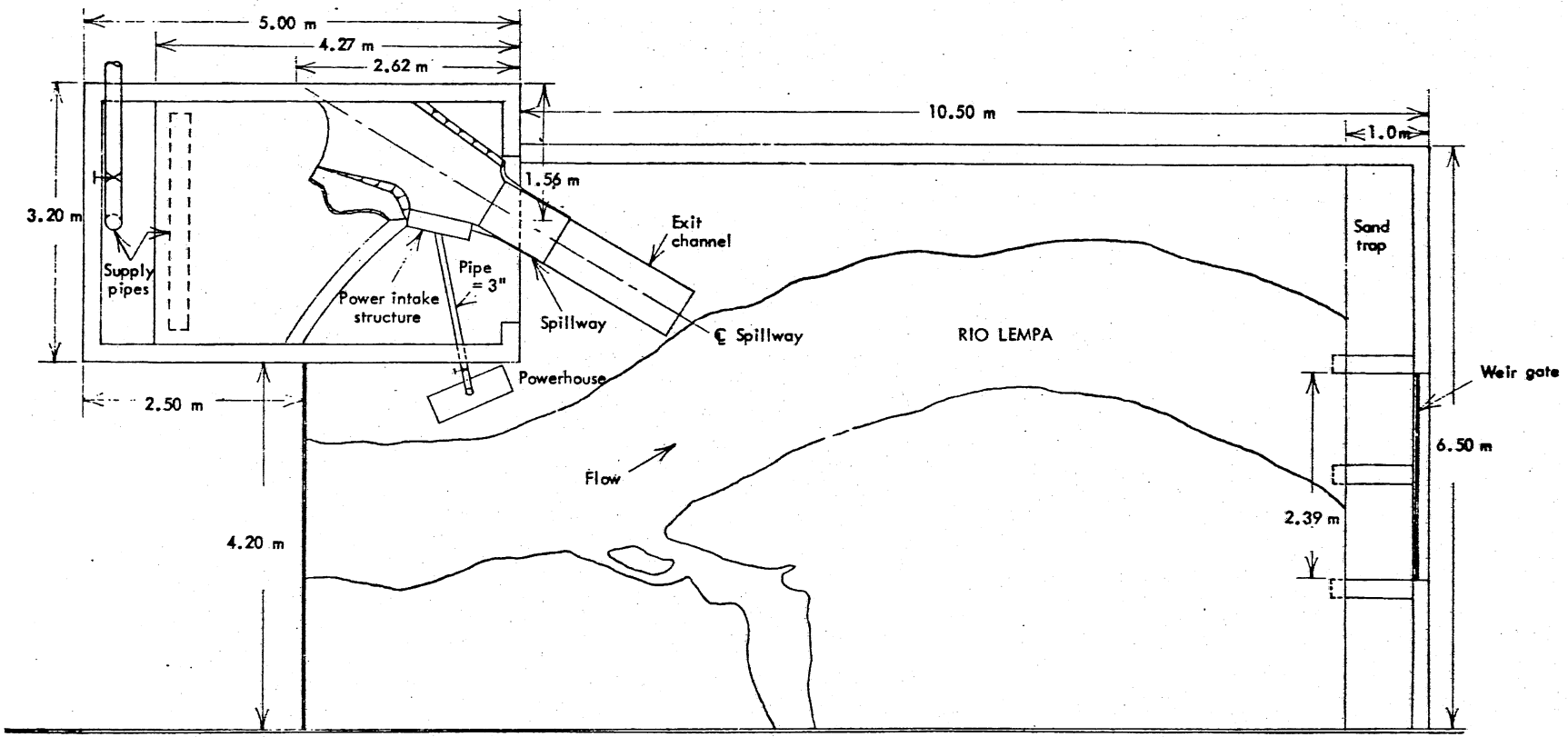

Fig. 1
GENERAL LAYOUT OF THE MODEL

SAINT ANTHONY FALLS HYDRAULIC LABORATORY
UNIVERSITY OF MINNESOTA

DRAWN	ECB	CHECKED	CCSS	APPROVED	
SCALE		DATE	1-15-73	NO	

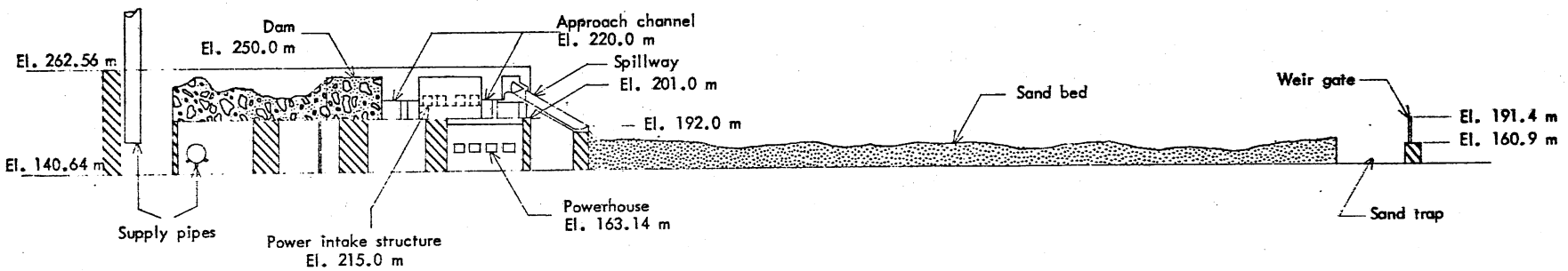

Fig. 2

TYPICAL CROSS SECTION
OF THE MODEL

SAINT ANTHONY FALLS HYDRAULIC LABORATORY
UNIVERSITY OF MINNESOTA

DRAWN ECB	CHECKED CCSS	APPROVED
SCALE	DATE 1-15-73	NO

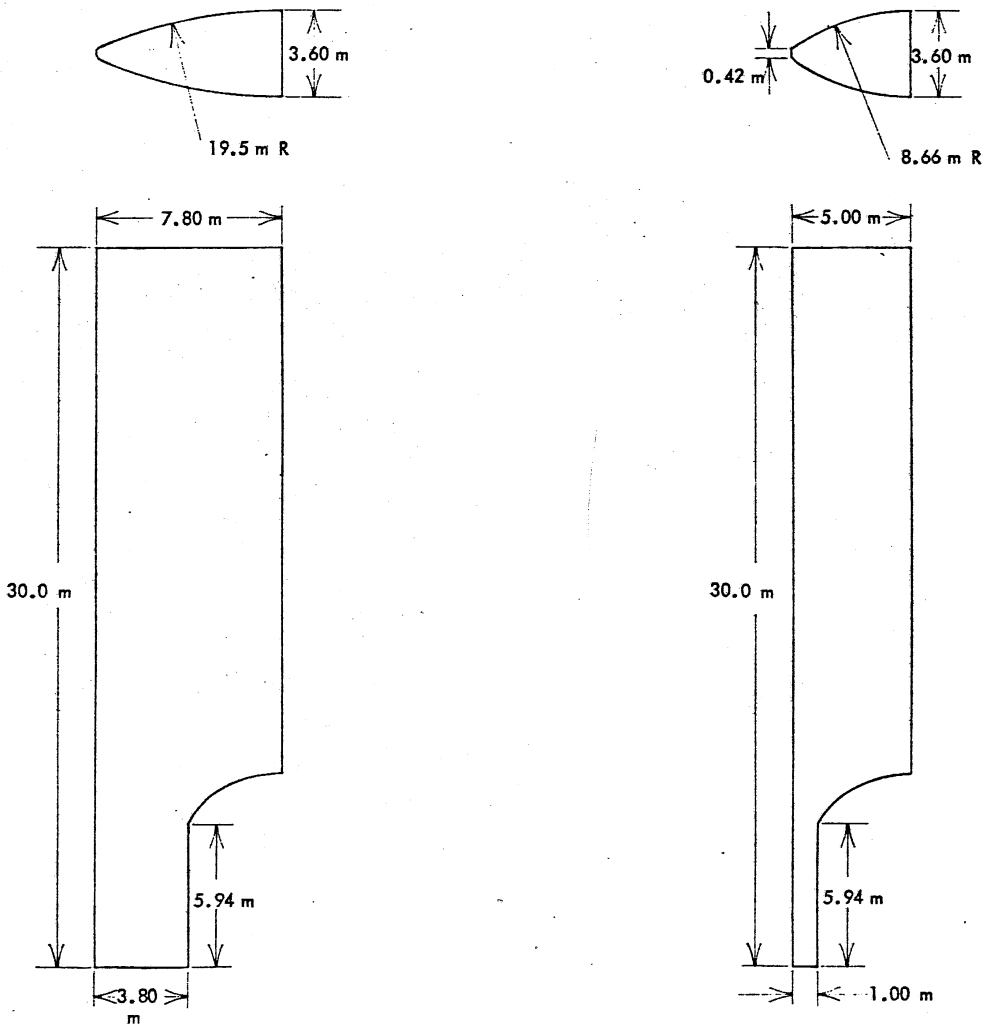

Fig. 3

CROSS SECTIONAL PROFILES OF PIER NOSES

SAINT ANTHONY FALLS HYDRAULIC LABORATORY
UNIVERSITY OF MINNESOTA

DRAWN ECB	CHECKED CCSS	APPROVED
SCALE	DATE 1-15-73	NO.

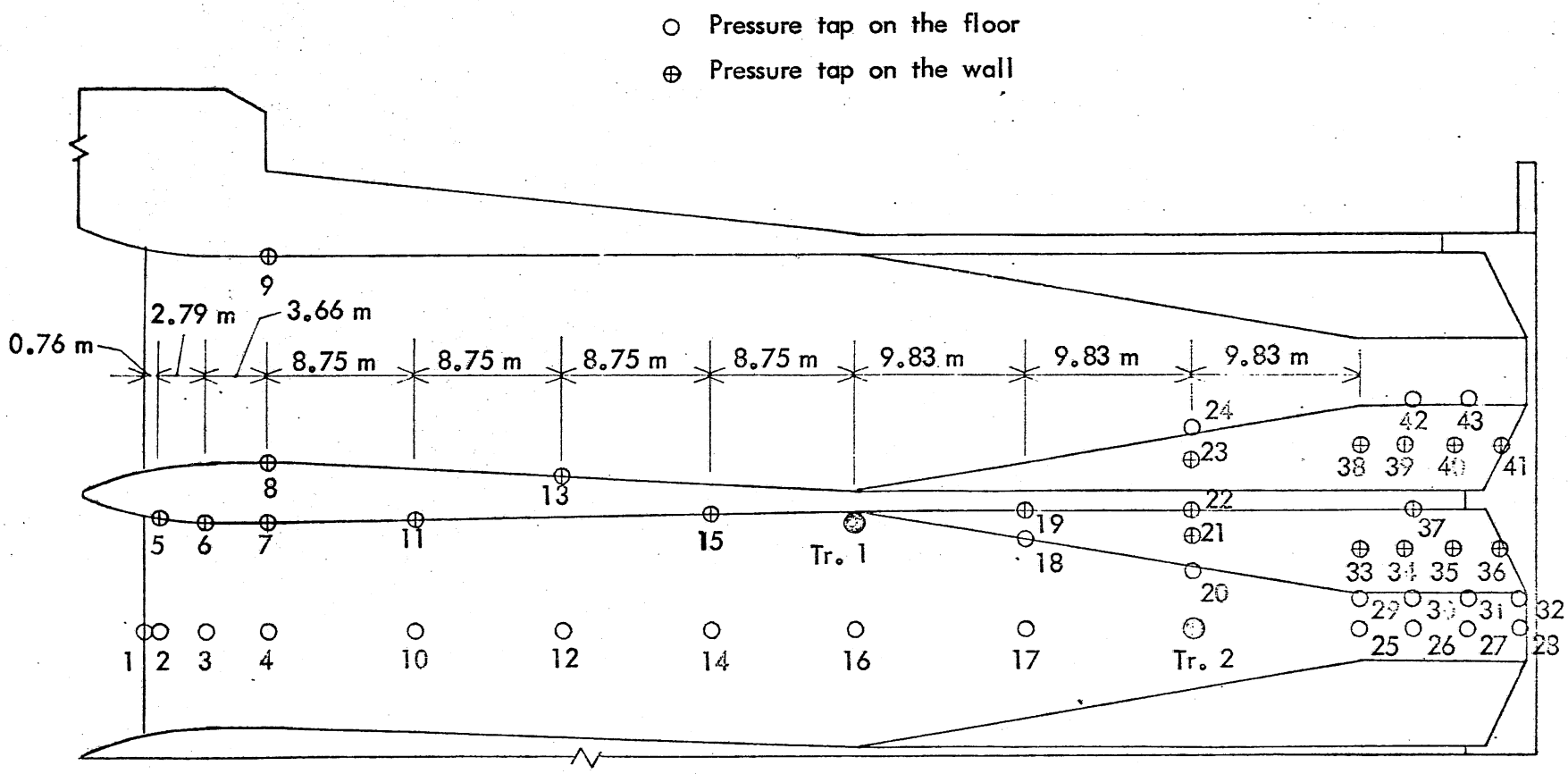

Fig. 4 - LOCATIONS OF PRESSURE TAPS AND TRANSDUCER OPENINGS

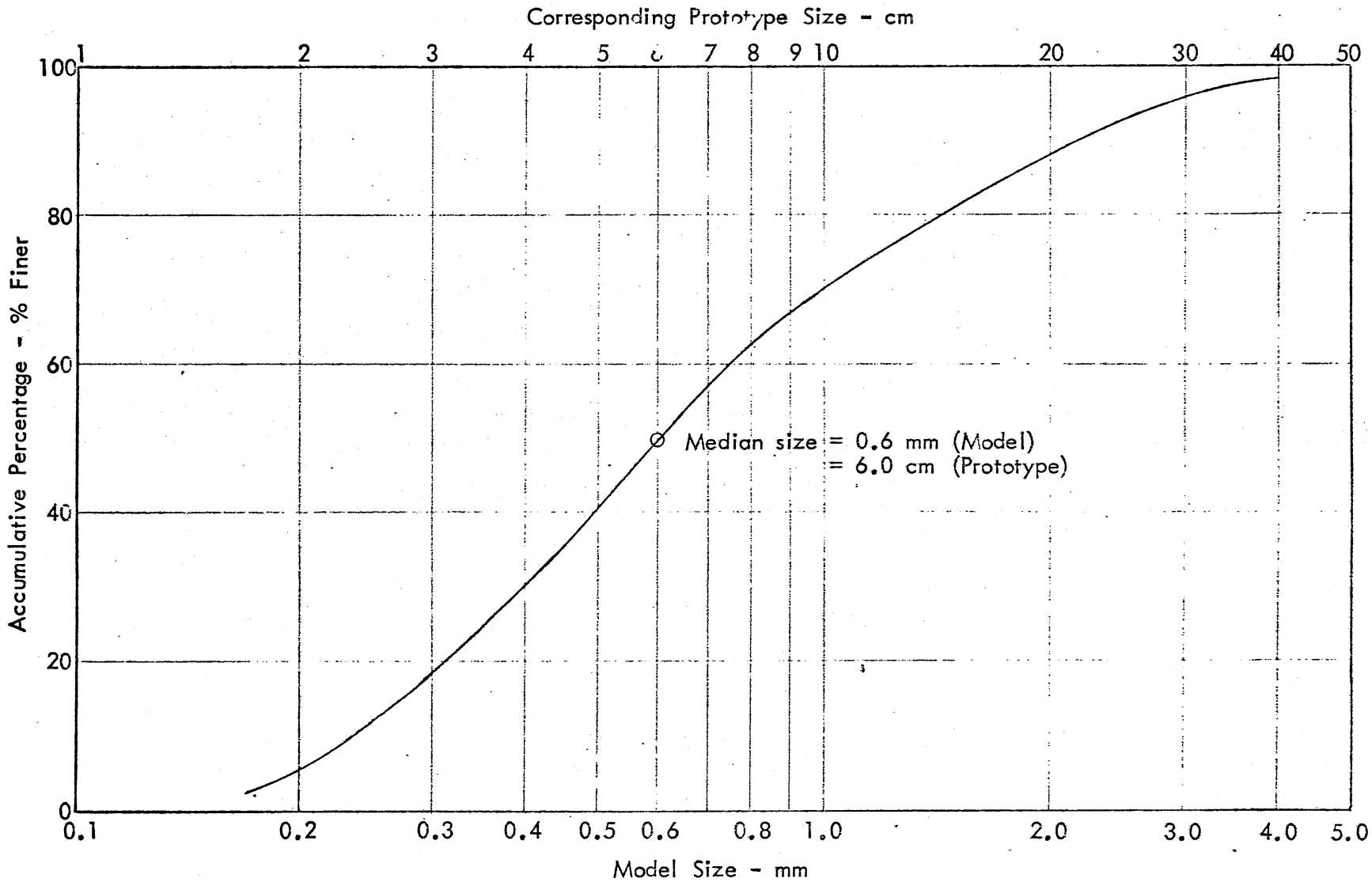

Fig. 5 - SIZE DISTRIBUTION OF SAND USED AS THE BED MATERIAL IN MODEL

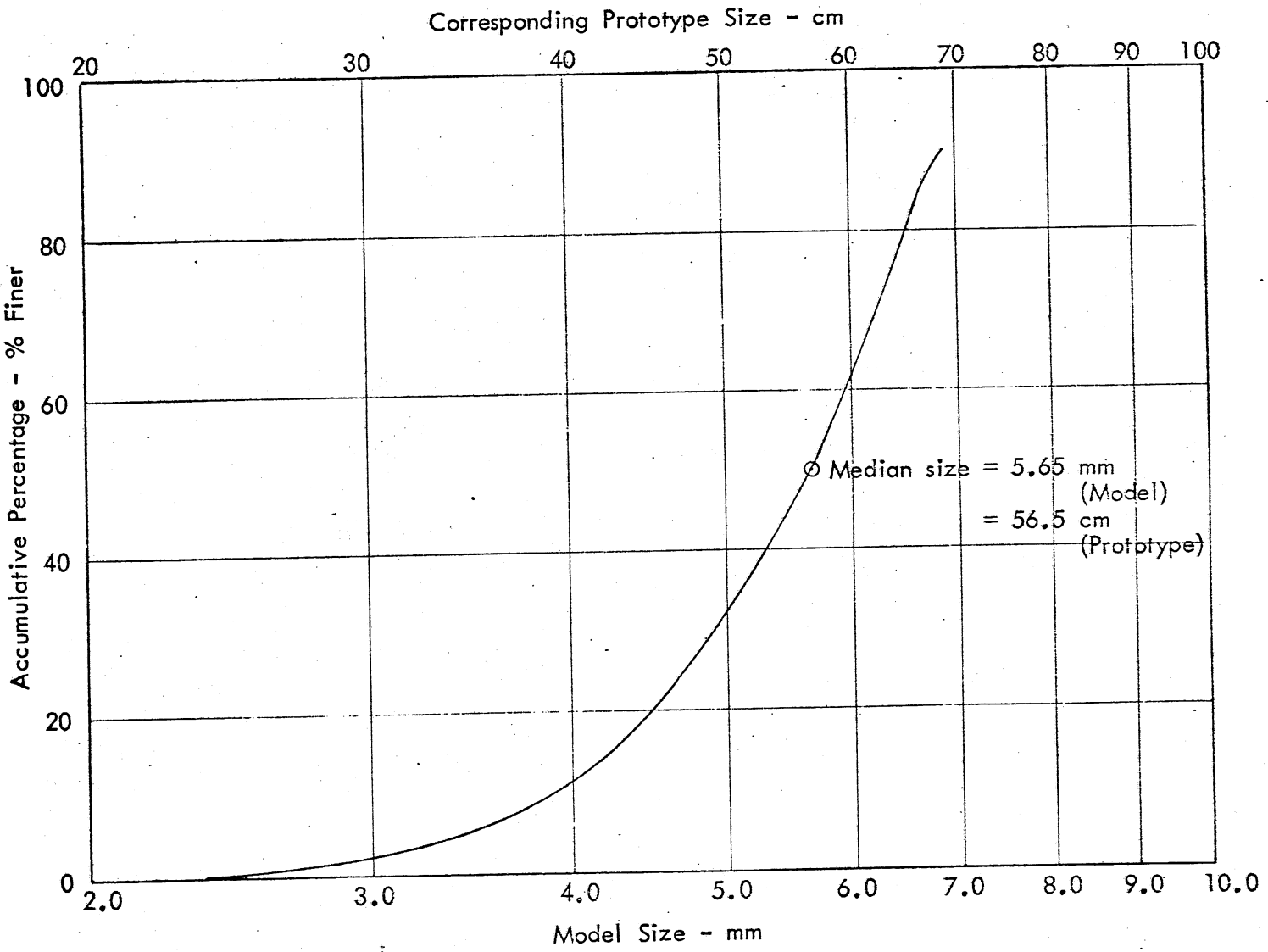

Fig. 6 - SIZE DISTRIBUTION OF GRAVEL USED IN THE EXIT CHANNEL

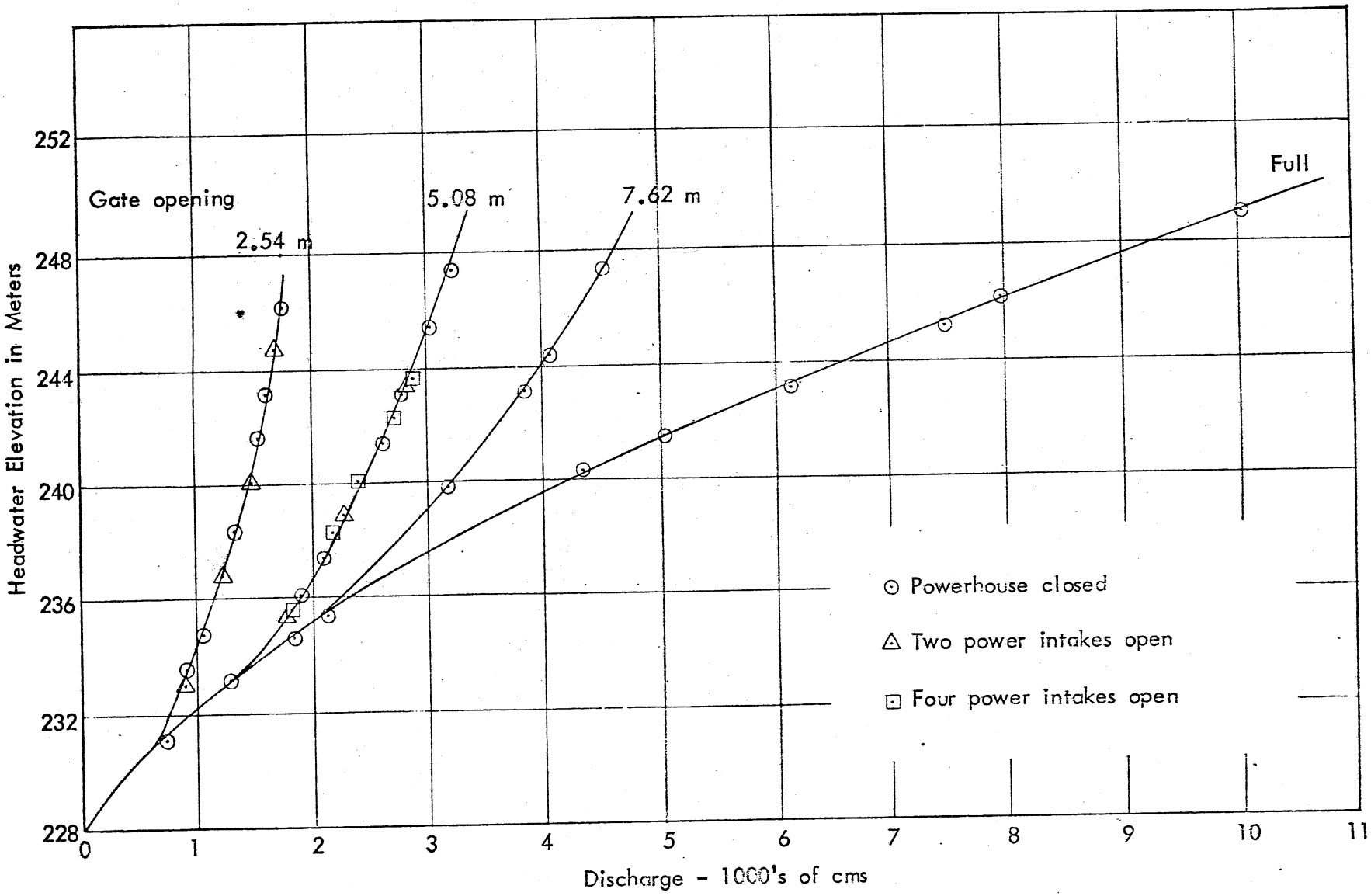

Fig. 7 - HEADWATER DISCHARGE RATING CURVES, DATA FOR FOUR GATES EQUALLY OPEN

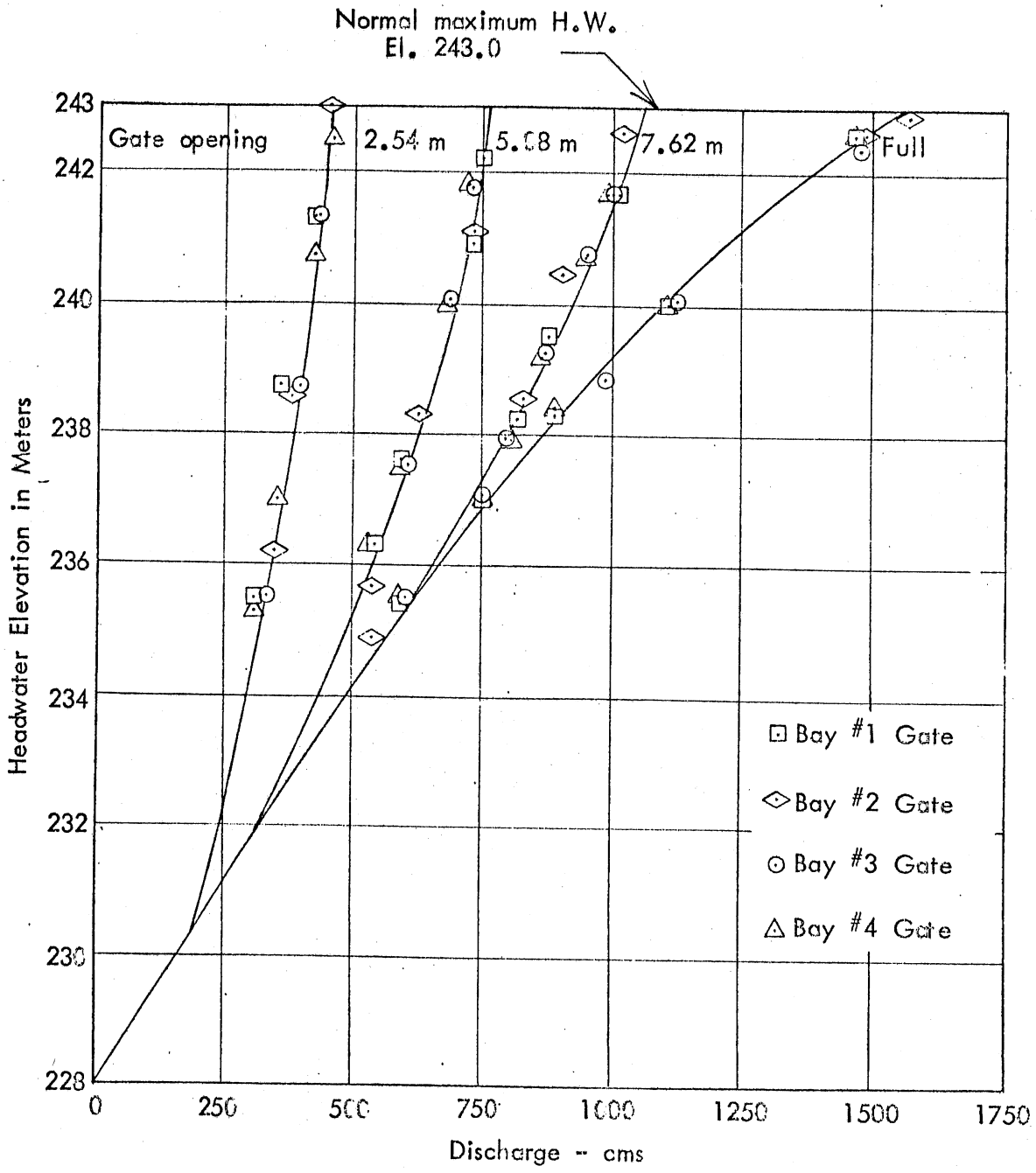

Fig. 8 - HEADWATER DISCHARGE RATING CURVES, DATA FOR SINGLE GATE OPERATION

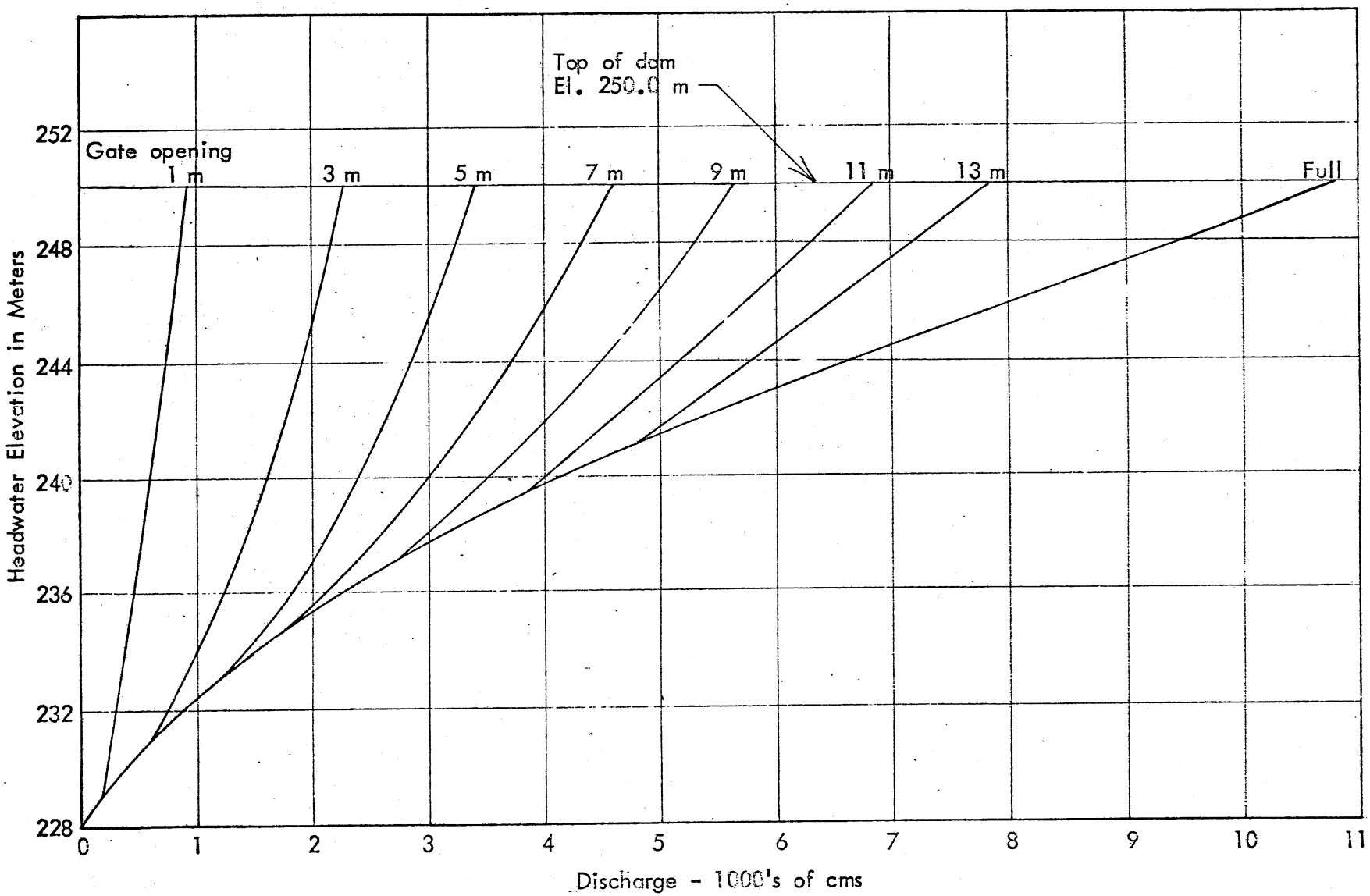

Fig. 9 - HEADWATER-DISCHARGE RATING CURVES, FOUR-GATE OPERATION

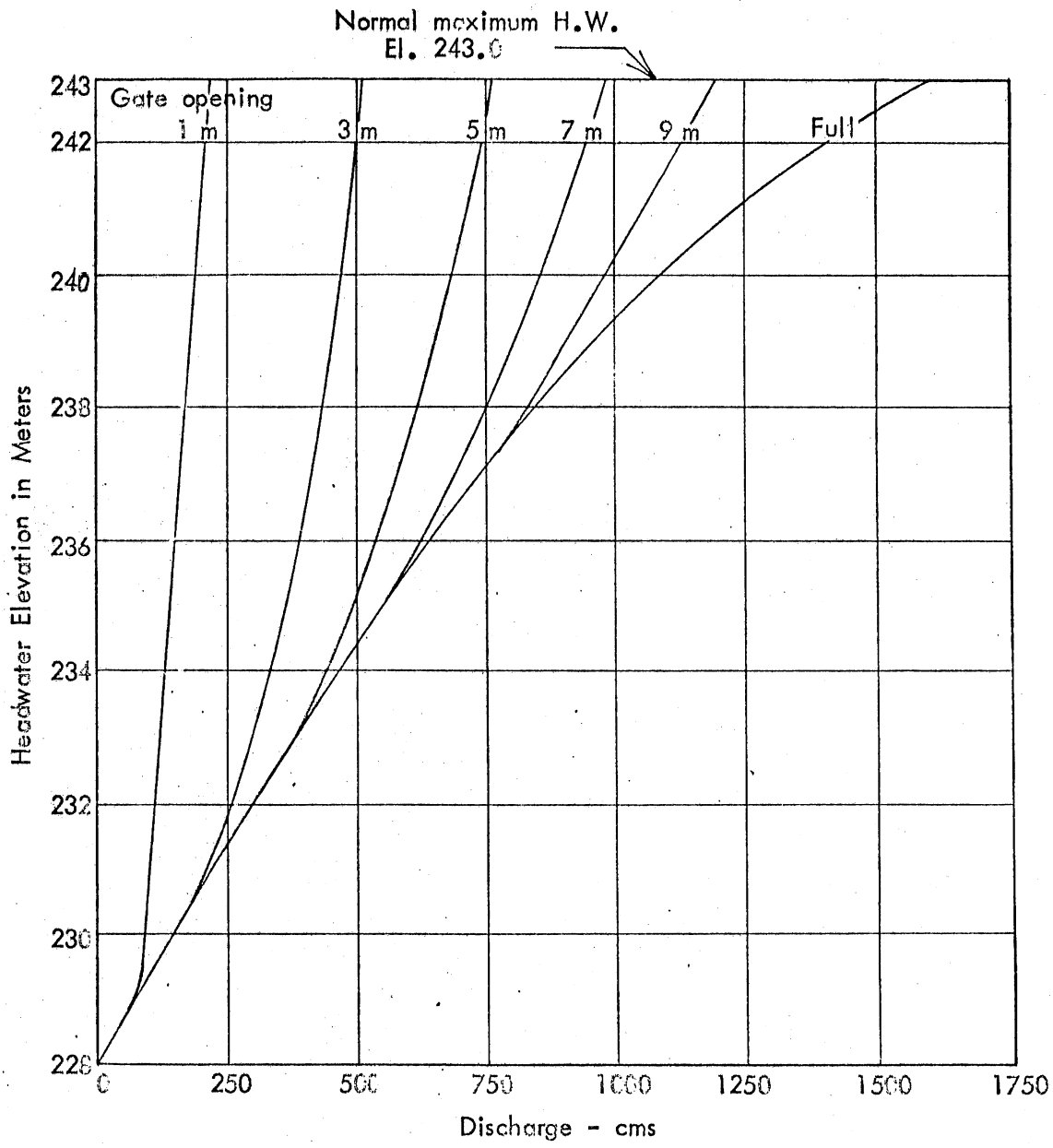

Fig. 10 - HEADWATER-DISCHARGE RATING CURVES, SINGLE-GATE OPERATION

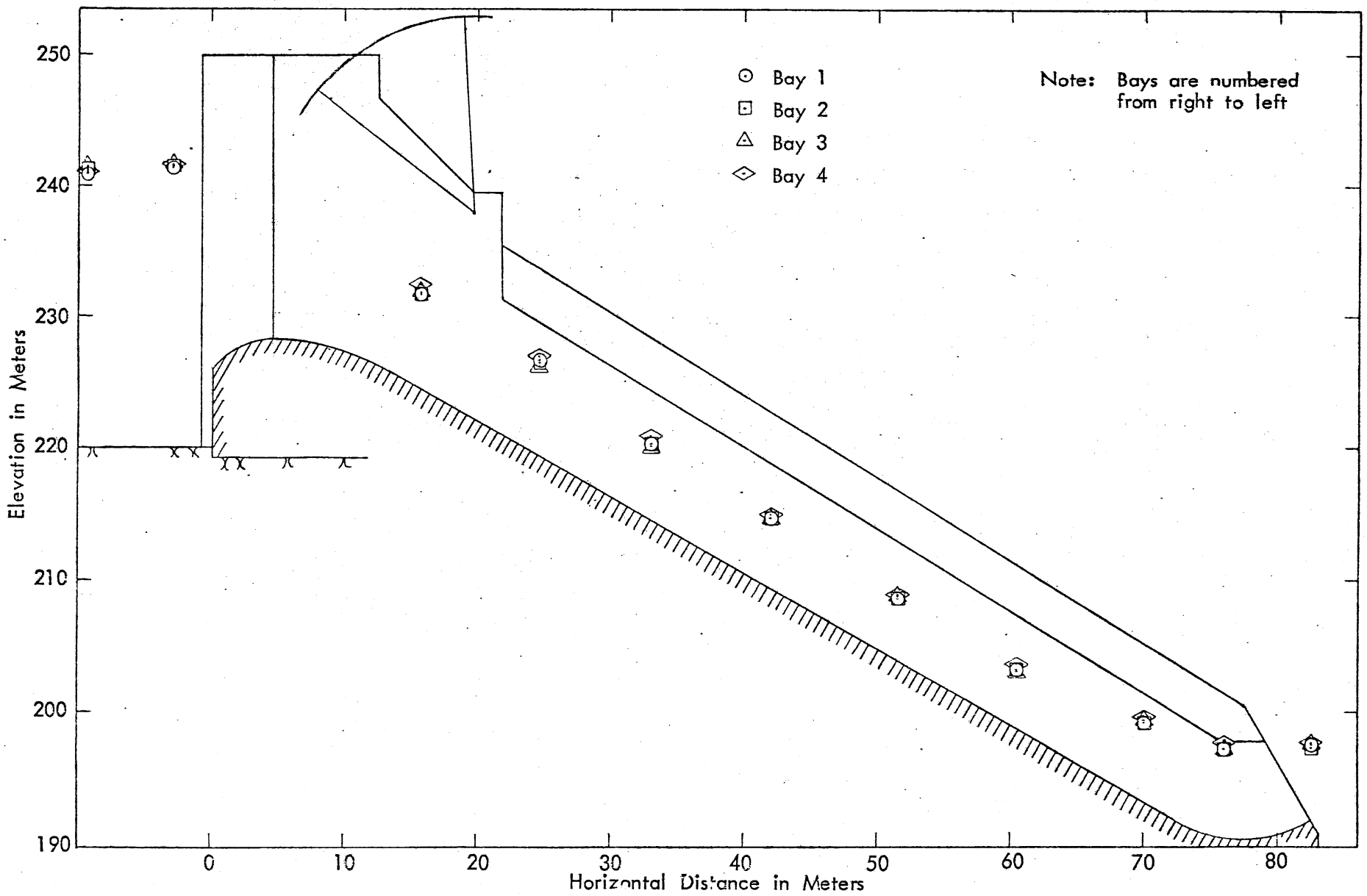

Fig. 11 - WATER SURFACE PROFILES ALONG CENTERLINE OF EACH BAY FOR NORMAL MAXIMUM DISCHARGE, Q = 5700 cms

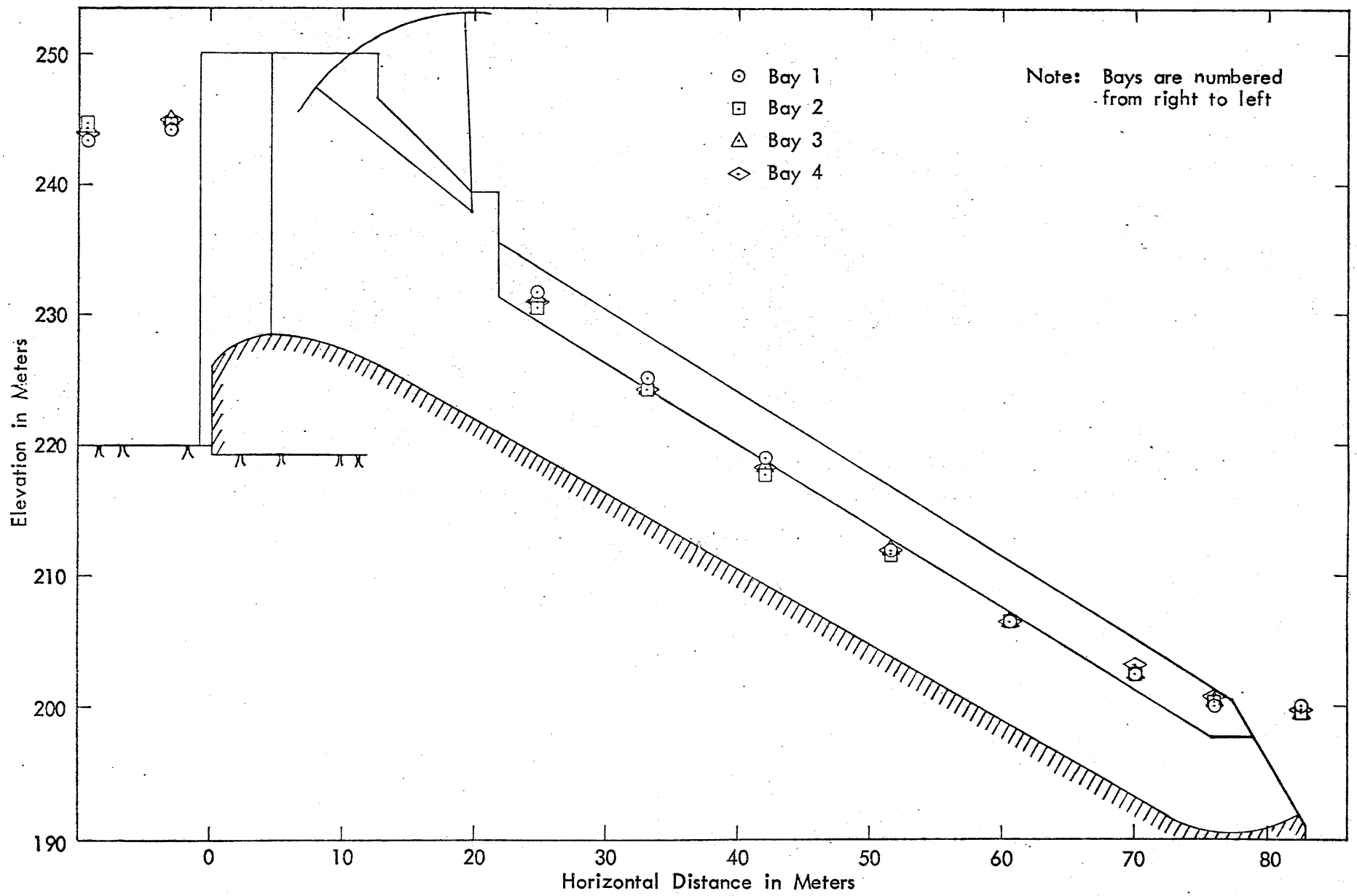

Fig. 12 - WATER SURFACE PROFILES ALONG CENTERLINE OF EACH BAY FOR MAXIMUM DISCHARGE, Q = 10,000 cms

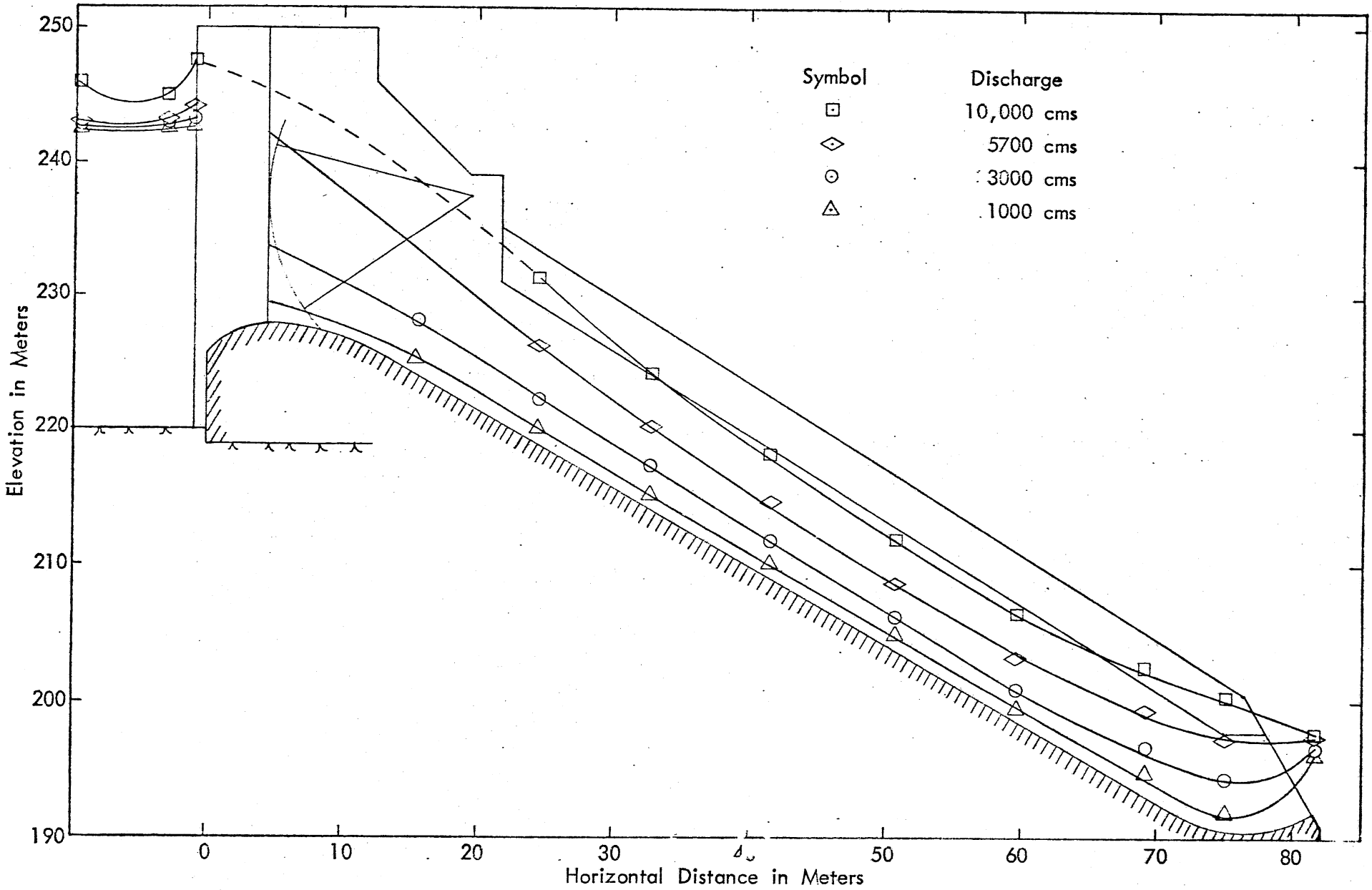

Fig. 13 - WATER SURFACE PROFILES ON THE CENTERLINES OF SPILLWAY BAYS

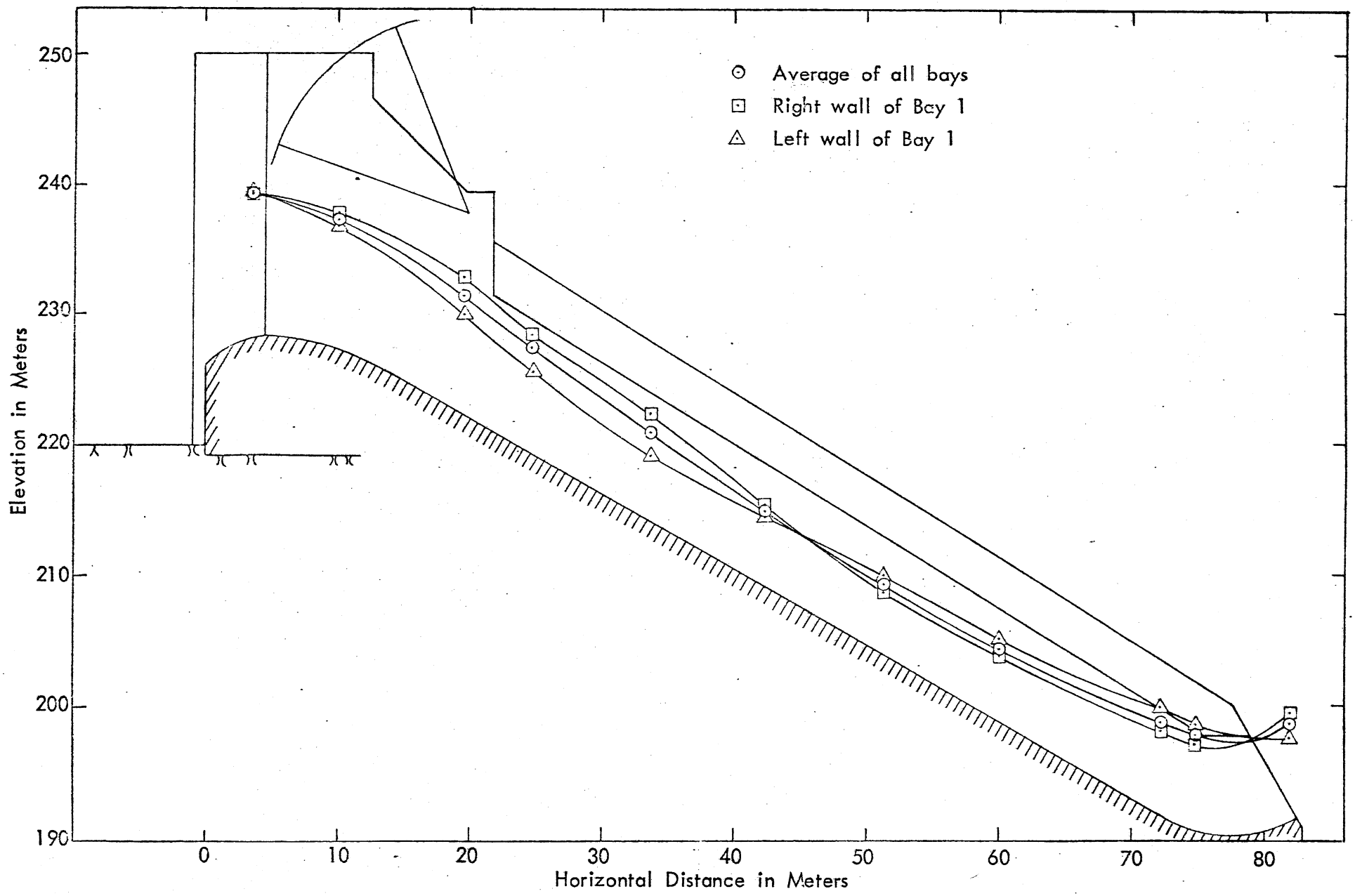

Fig. 14 - WATER SURFACE PROFILES ALONG WALLS FOR NORMAL MAXIMUM DISCHARGE, Q = 5700 cms

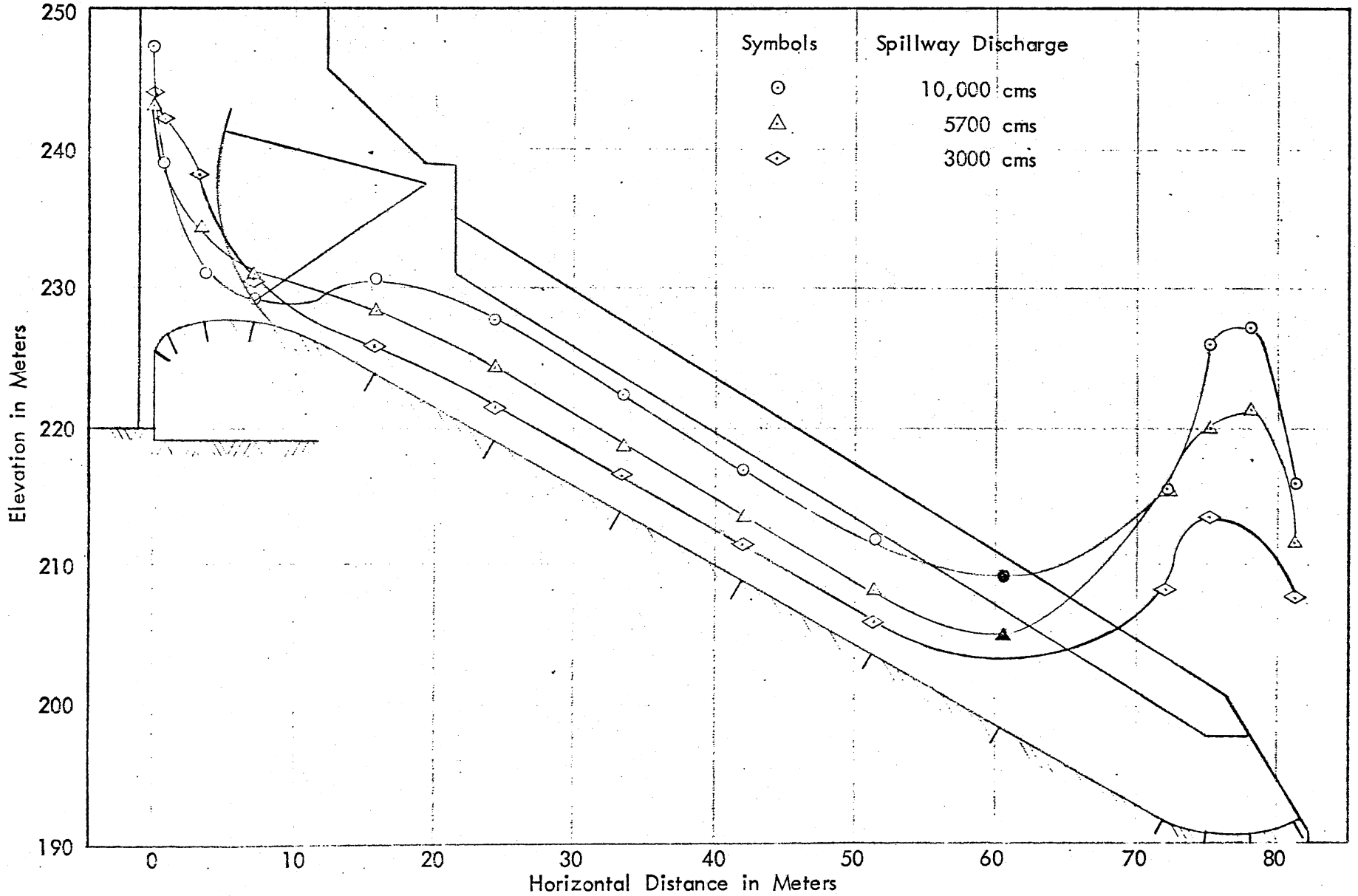

Fig. 15 - PRESSURE DISTRIBUTION ALONG CENTERLINE OF THE SPILLWAY SURFACE

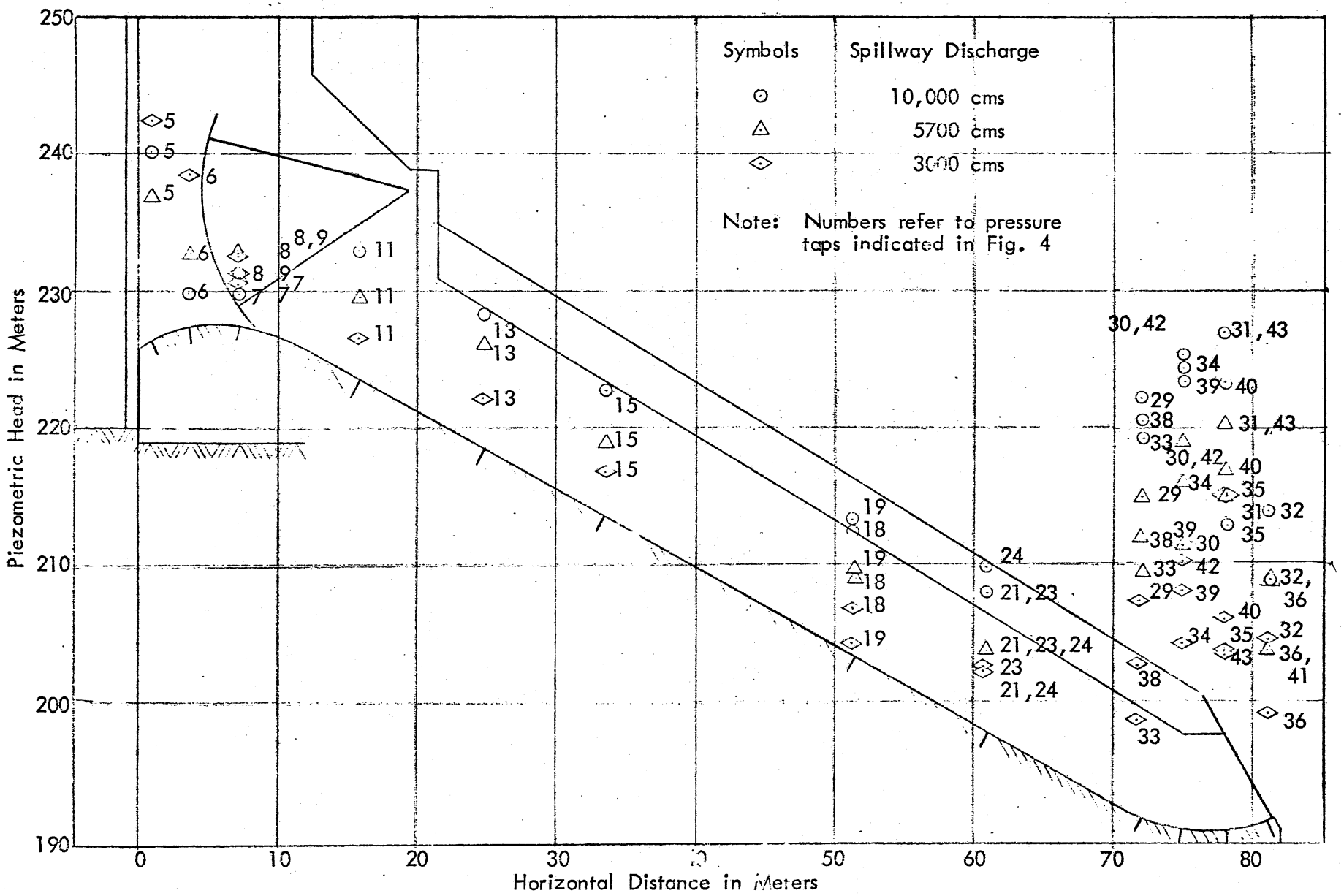

Fig. 16 - PRESSURE DISTRIBUTION ON WALLS AND OFF CENTERLINE OF THE SPILLWAY SURFACE

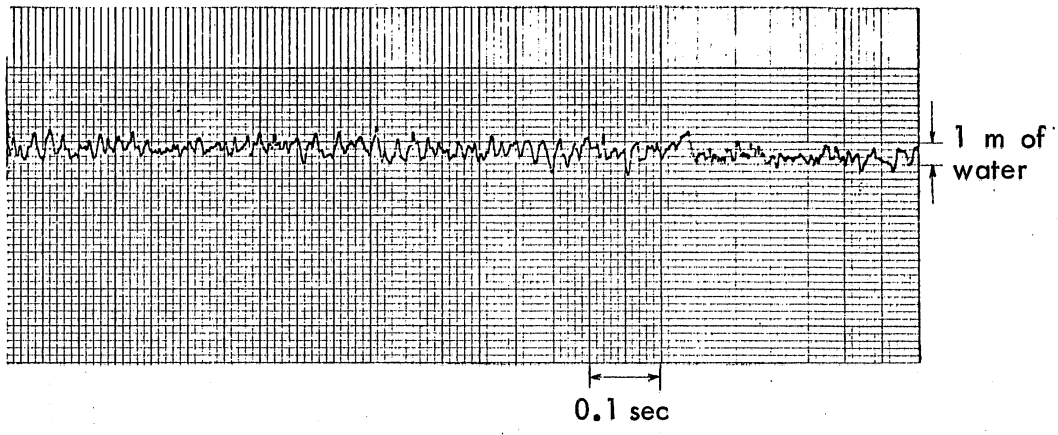

(a) Q = 5700 cms

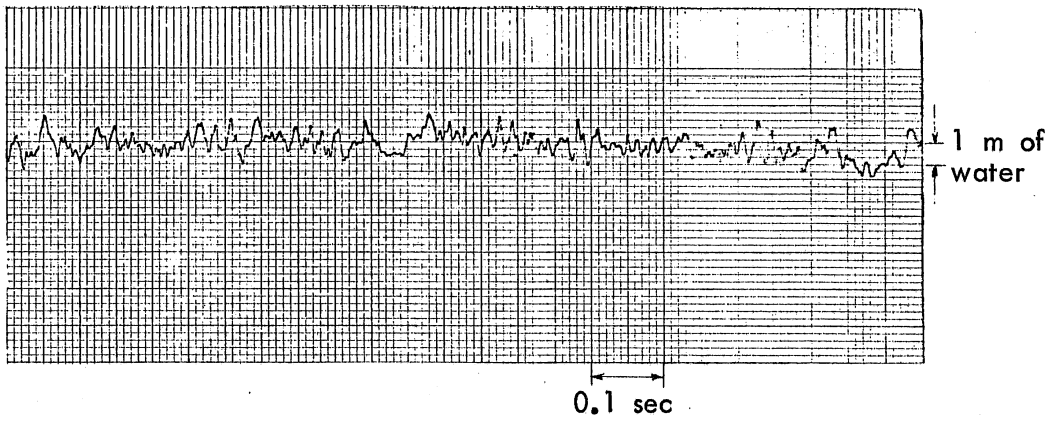

(b) Q = 10,000 cms

Fig. 17 - SAMPLE PRESSURE MEASUREMENT RECORDS OBTAINED WITH NO. 2 PRESSURE TRANSDUCER

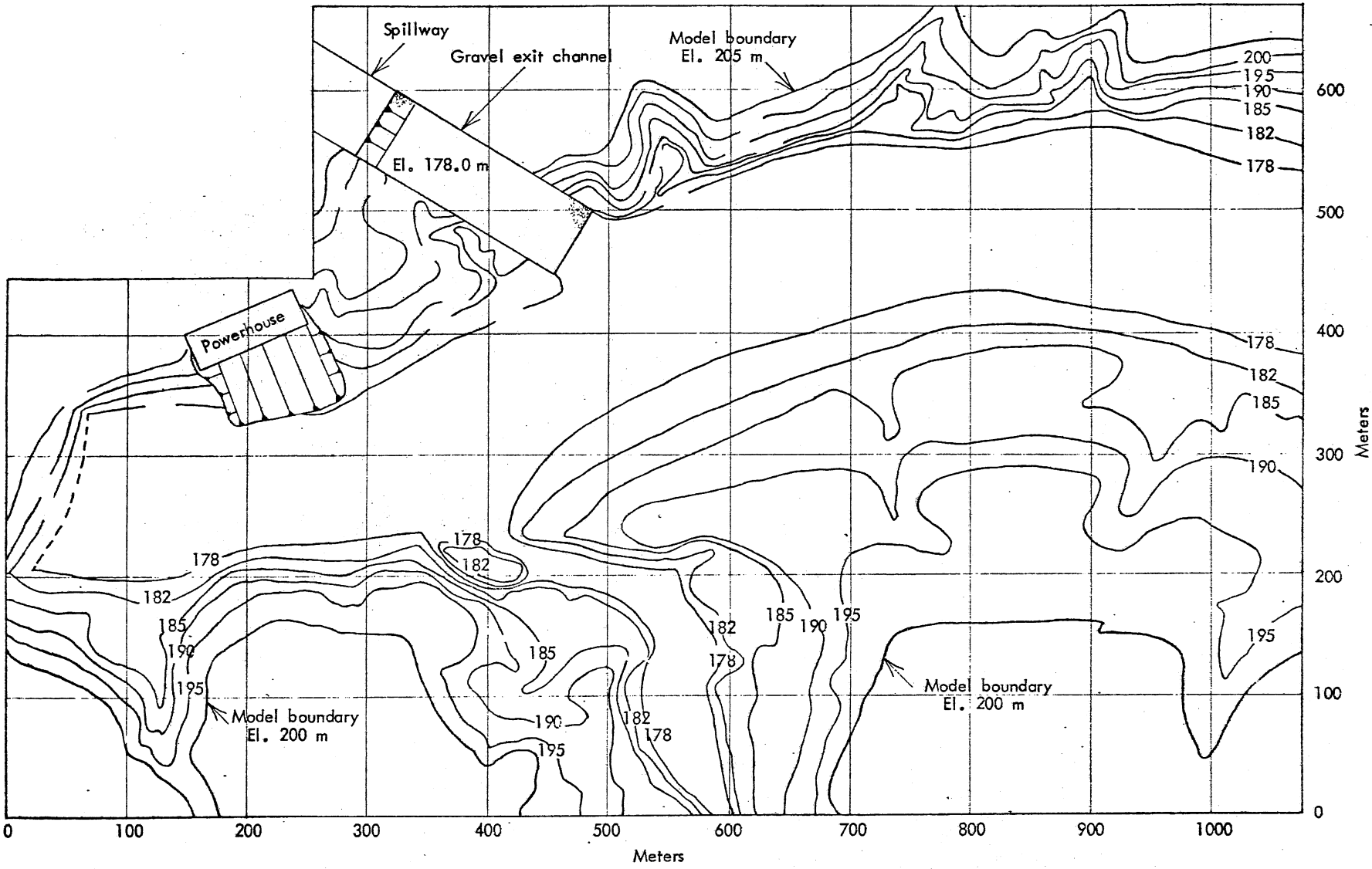

Fig. 18 - INITIAL TOPOGRAPHY DOWNSTREAM OF SPILLWAY AND POWERHOUSE

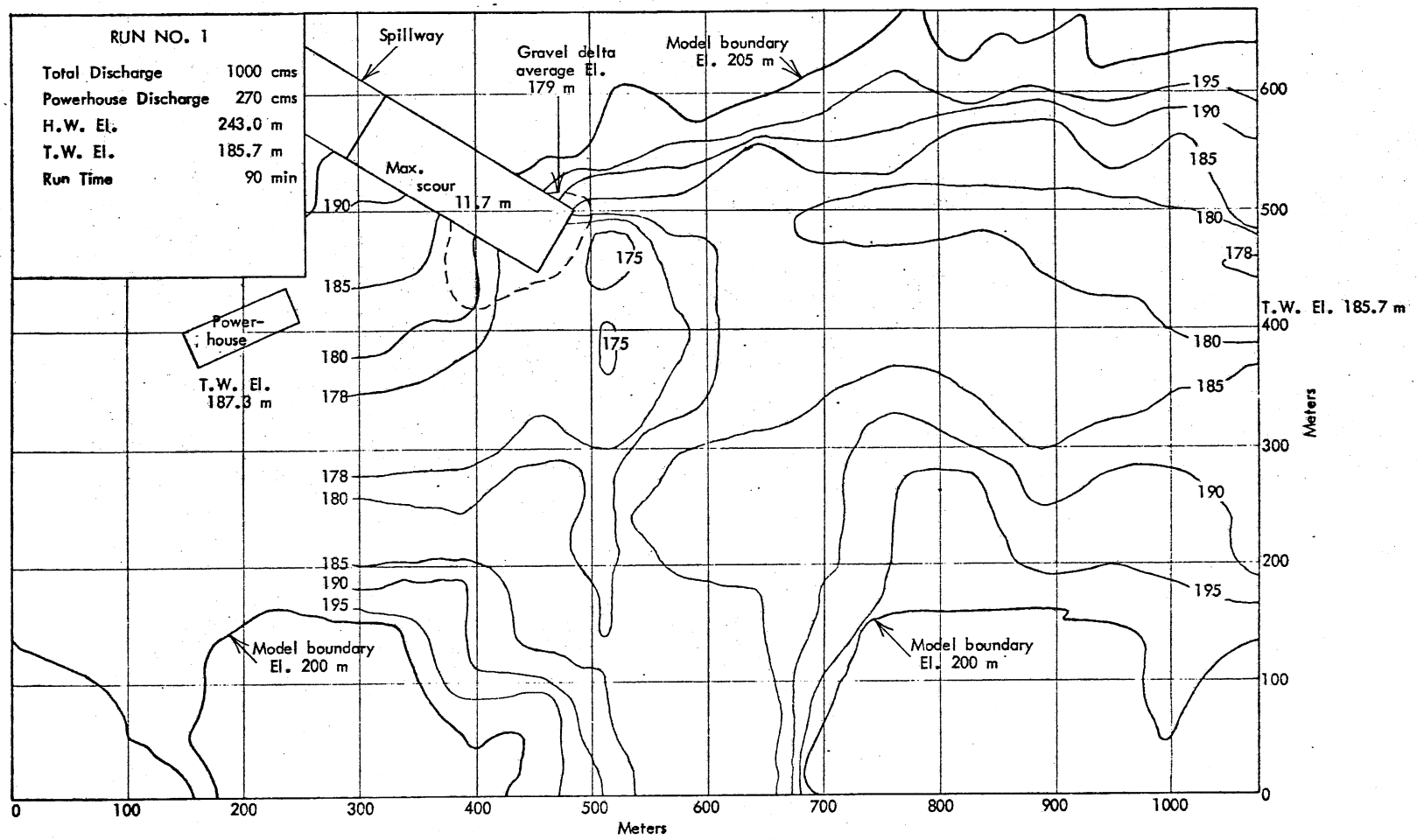

Fig. 19 - TAILRACE EROSION PATTERN - GRAVEL EXIT CHANNEL - RUN NO. 1

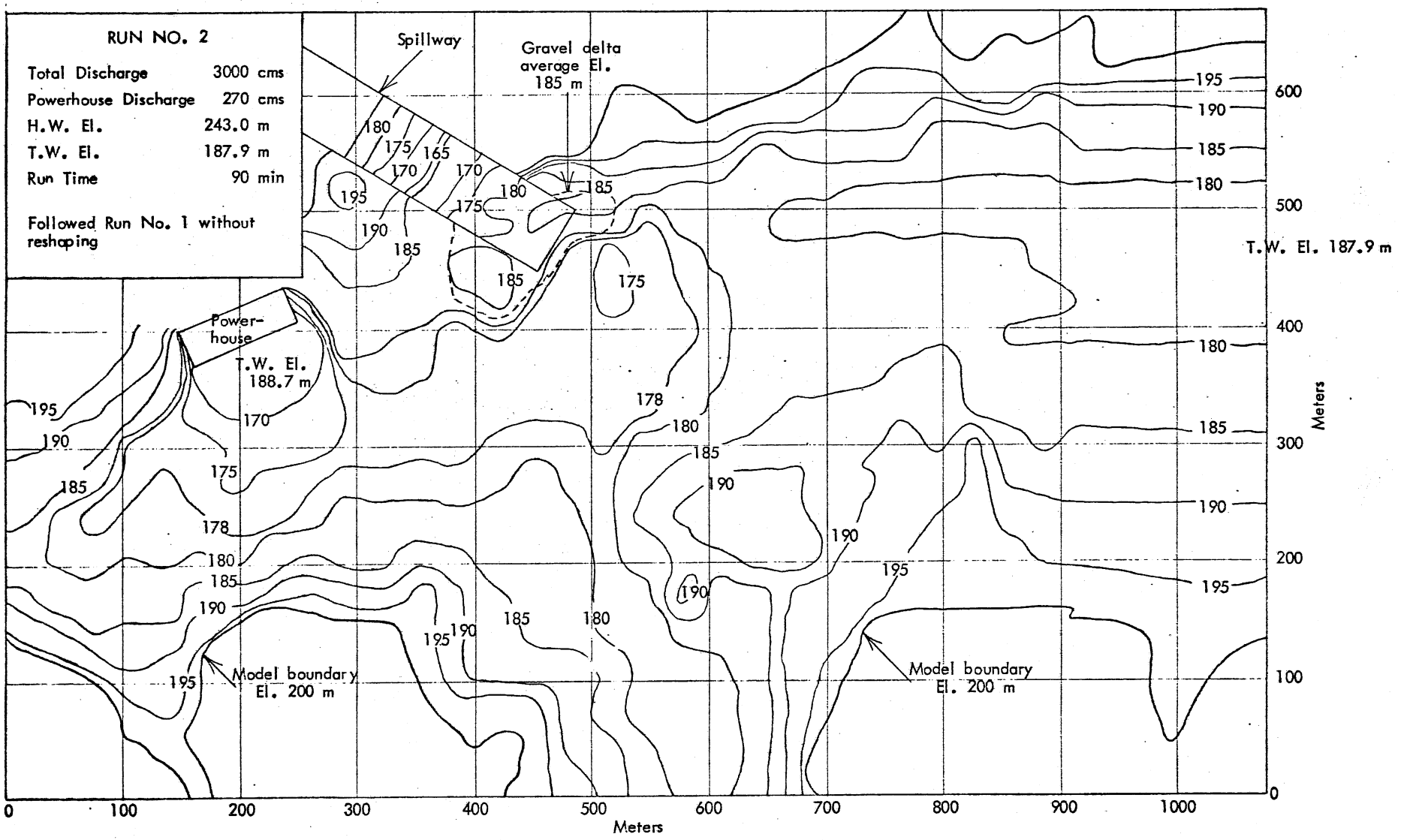

Fig. 20 - TAILRACE EROSION PATTERN - GRAVEL EXIT CHANNEL - RUN NO. 2

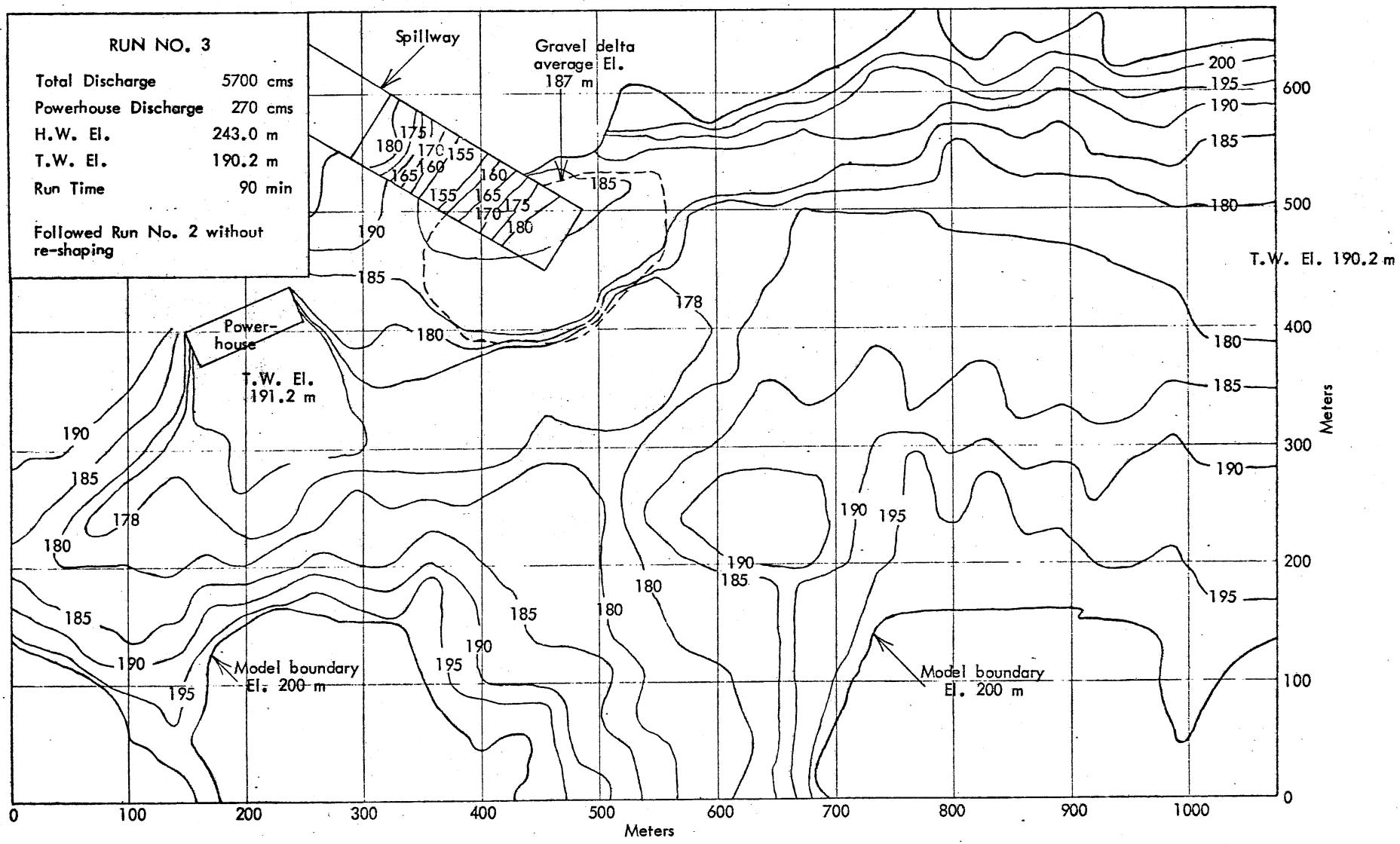

Fig. 21 - TAILRACE EROSION PATTERN - GRAVEL EXIT CHANNEL - RUN NO. 3

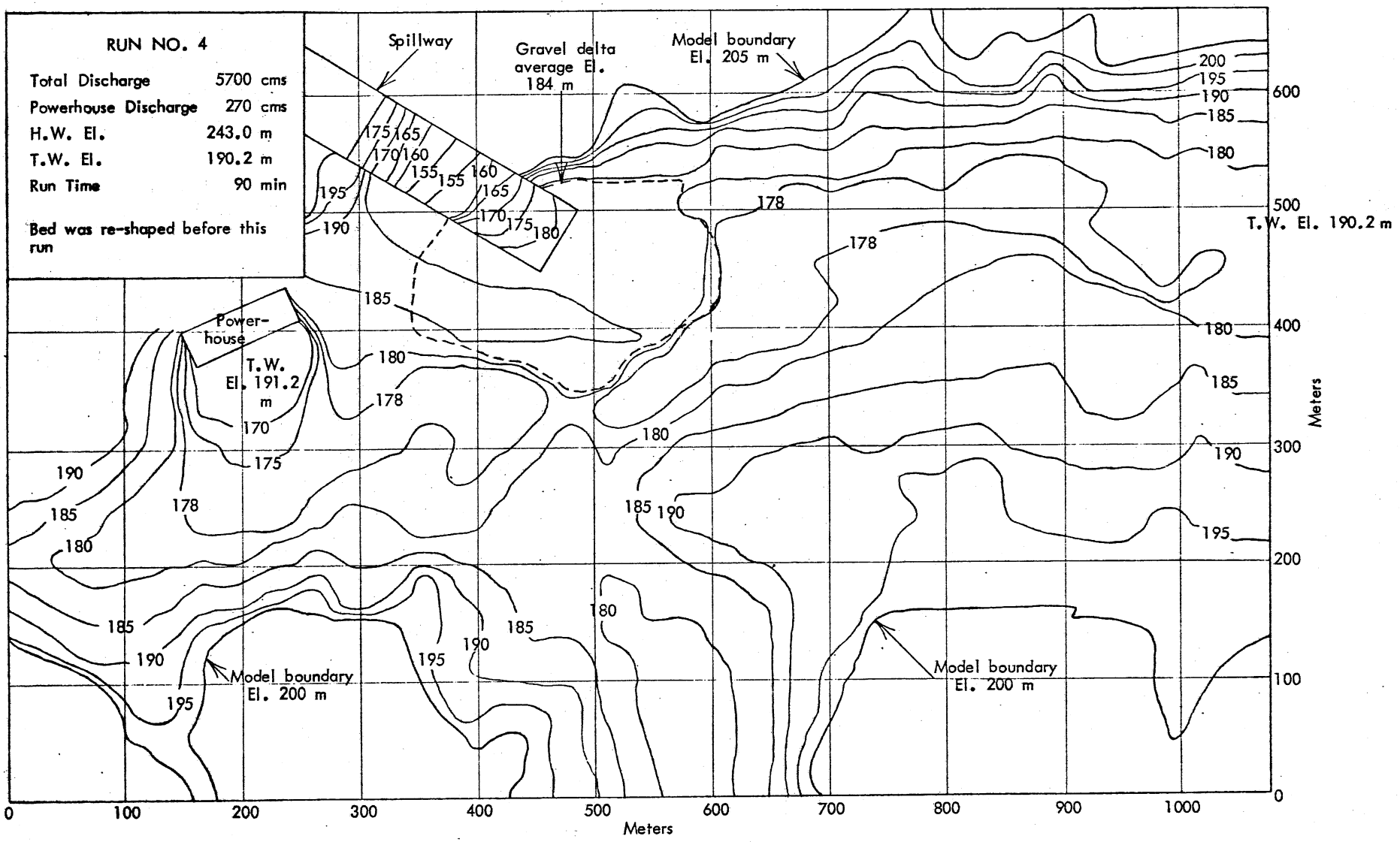

Fig. 22 - TAILRACE EROSION PATTERN - GRAVEL EXIT CHANNEL - RUN NO. 4

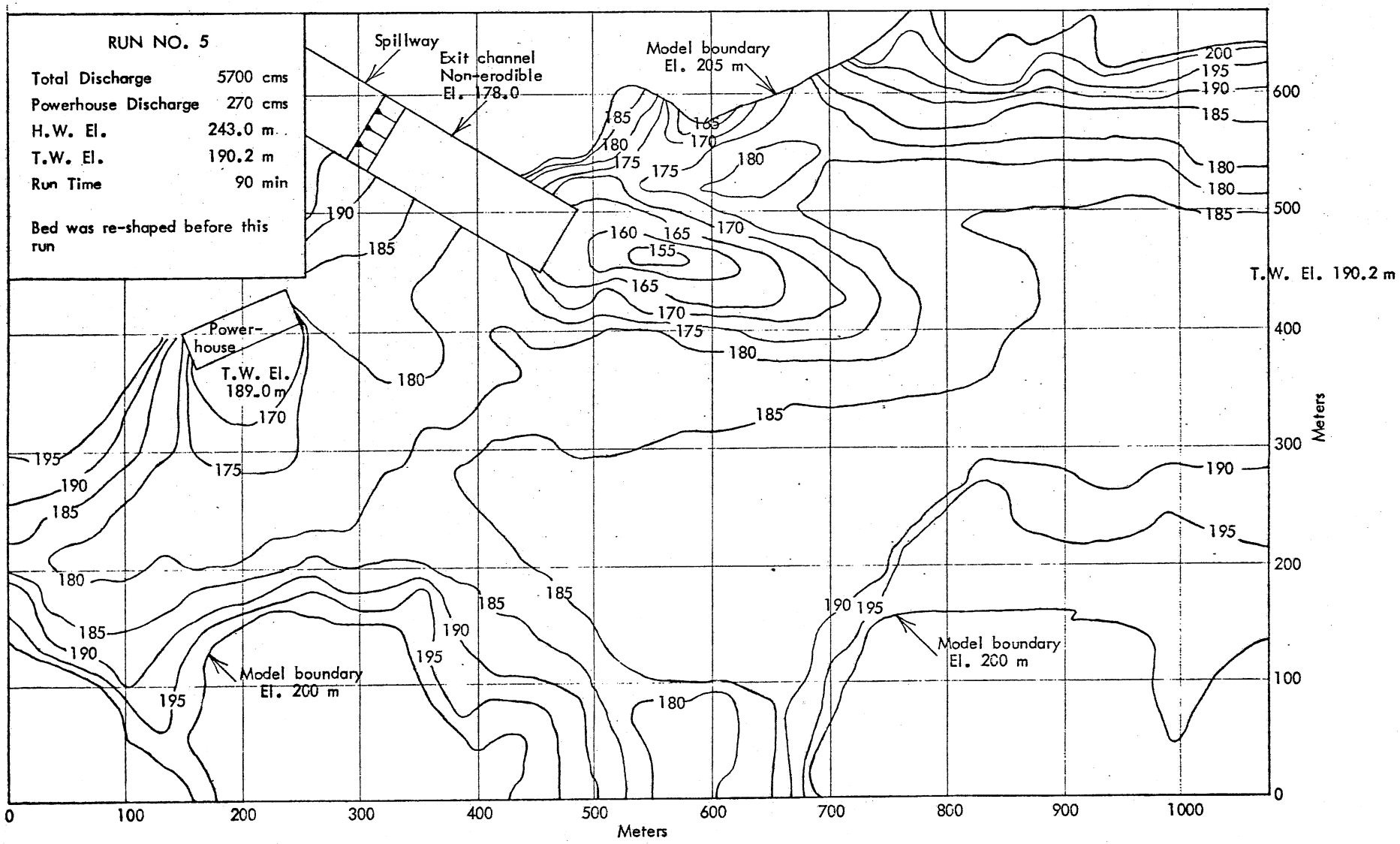

Fig. 23 - TAILRACE EROSION PATTERN WITH NON-ERODIBLE EXIT CHANNEL AFTER 90 MINUTES AT Q = 5700 cms

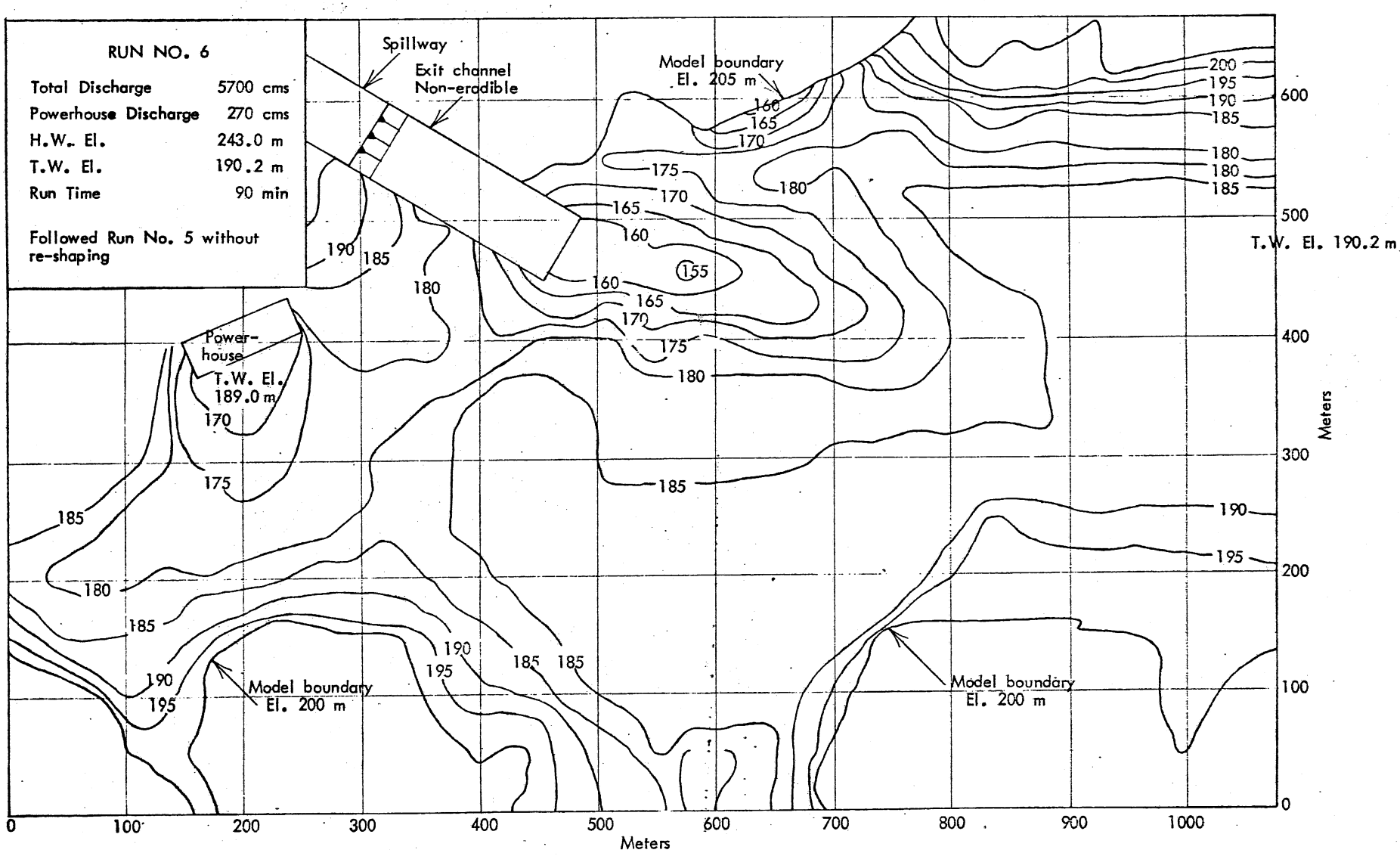

Fig. 24 - TAILRACE EROSION PATTERN WITH NON-ERODIBLE EXIT CHANNEL AFTER 180 MINUTES AT Q = 5700 cms

LIST OF PHOTOS

Photo No.	
1	General View of the Model
2	View of the Spillway Model
3	Surface Flow Pattern in Approach Channel, Q = 1000 cms
4	Surface Flow Pattern in Approach Channel, Q = 3000 cms
5	Surface Flow Pattern in Approach Channel, Q = 5700 cms
6	Surface Flow Pattern in Approach Channel, Q = 10,000 cms
7	Vortex Pair at Spillway Gate, Q = 850 cms
8	Scour in Exit Channel and Delta, Q = 1000 cms
9	Scour in Exit Channel and Delta, Q = 3000 cms
10	Scour in Exit Channel and Delta, Q = 5700 cms
11	View of Erosion Pattern after 90 minute run at Q = 5700 cms with Erodible Exit Channel
12	View of Powerhouse Exit after a run with Q = 5700 cms
13	Downstream view of Spillway Flow at Q = 5700 cms with Concrete Exit Channel, very little lateral spreading and energy dissipation
14	Large Clockwise-rotating Vortex generated by the Spillway Discharge when Concrete Bed is used for Exit Channel
15	Very Intensive Counterclockwise-rotating Vortex generated by the Spillway Discharge when Concrete Bed is used for Exit Channel
16	Scouring Immediately Downstream of Concrete Exit Channel after 90 minutes of discharge at 5700 cms
17	Sand Bar to the right of the Main Flow formed by the Clockwise-rotating Vortex

Photo 1 - General View of the Model

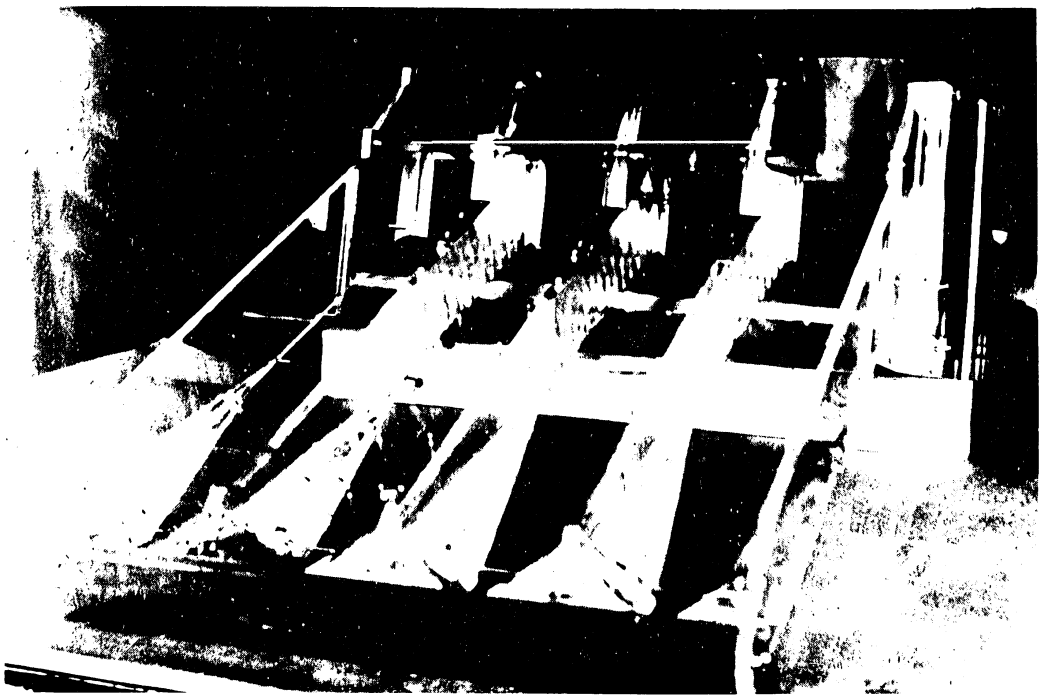

Photo 2 - View of the Spillway Model

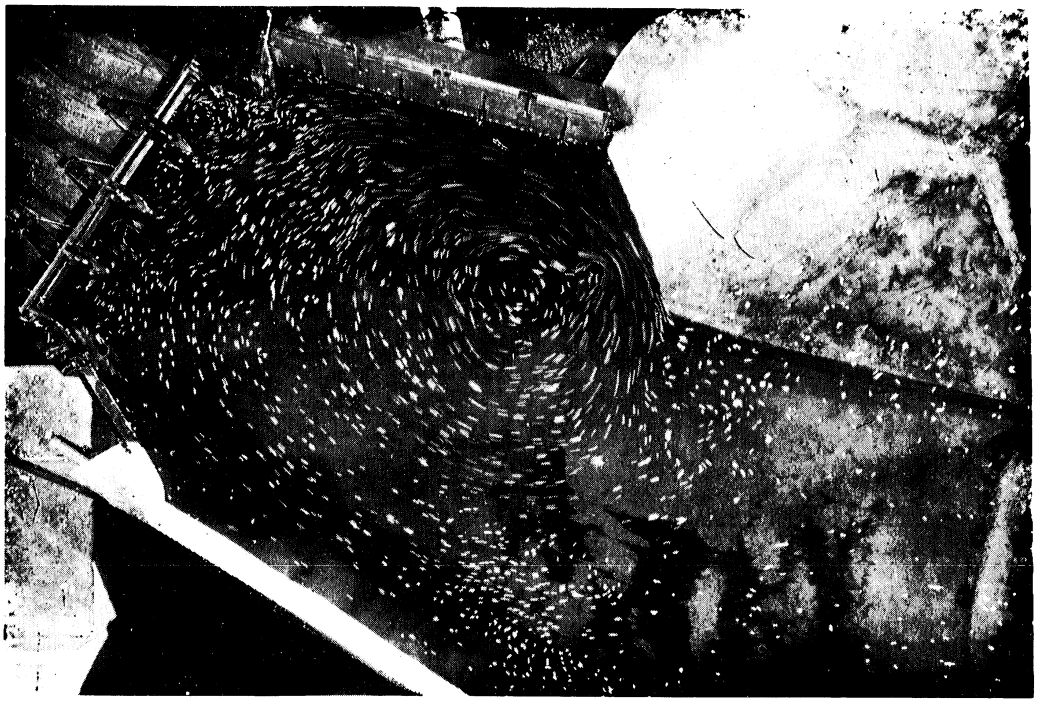

Photo 3 - Surface Flow Pattern in Approach Channel, Q = 1000 cms

Photo 4 - Surface Flow Pattern in Approach Channel, Q = 3000 cms

Photo 5 - Surface Flow Pattern in Approach Channel, Q = 5700 cms

Photo 6 - Surface Flow Pattern in Approach Channel, Q = 10,000 cms

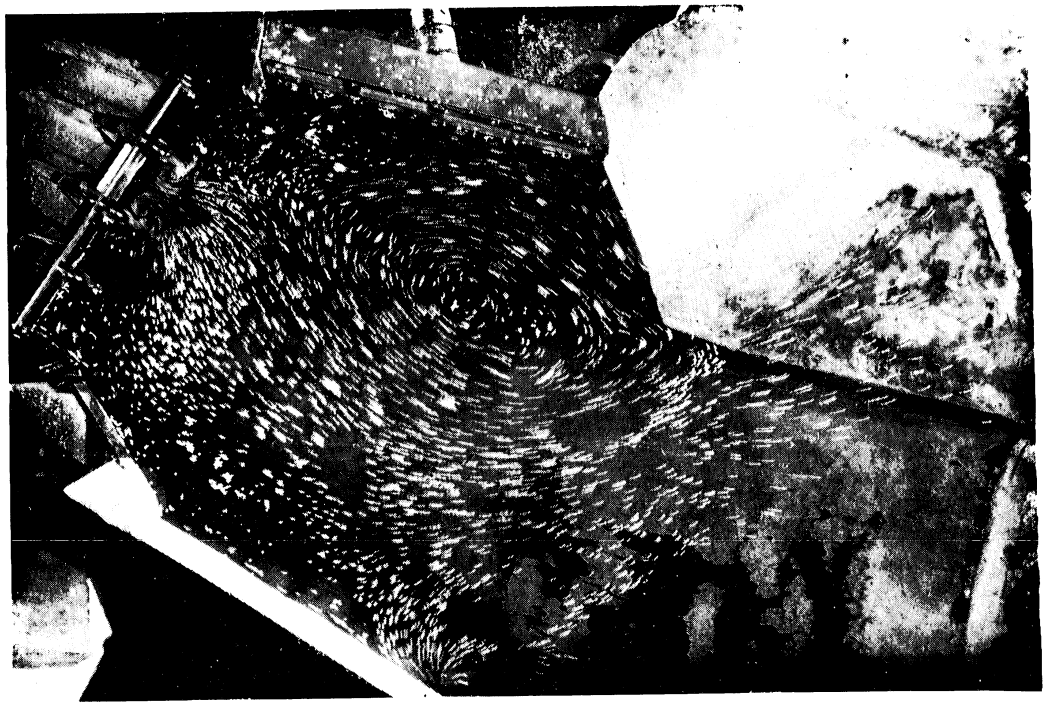

Photo 7 - Vortex Pair at Spillway Gate, Q = 850 cms

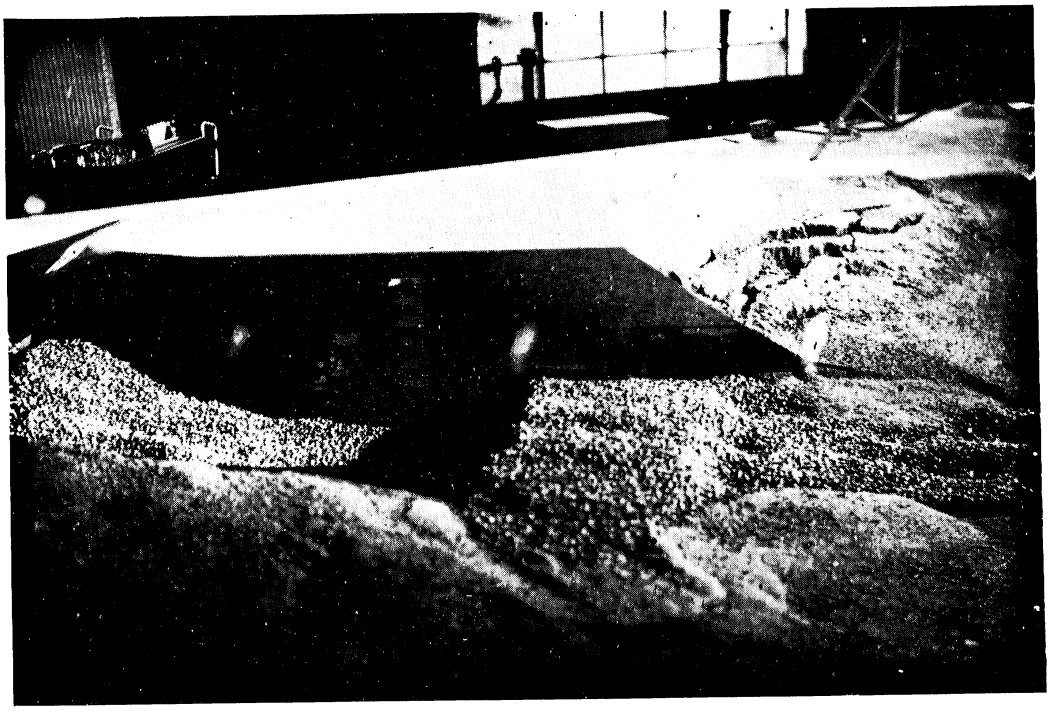

Photo 8 - Scour in Exit Channel and Delta, Q = 1000 cms

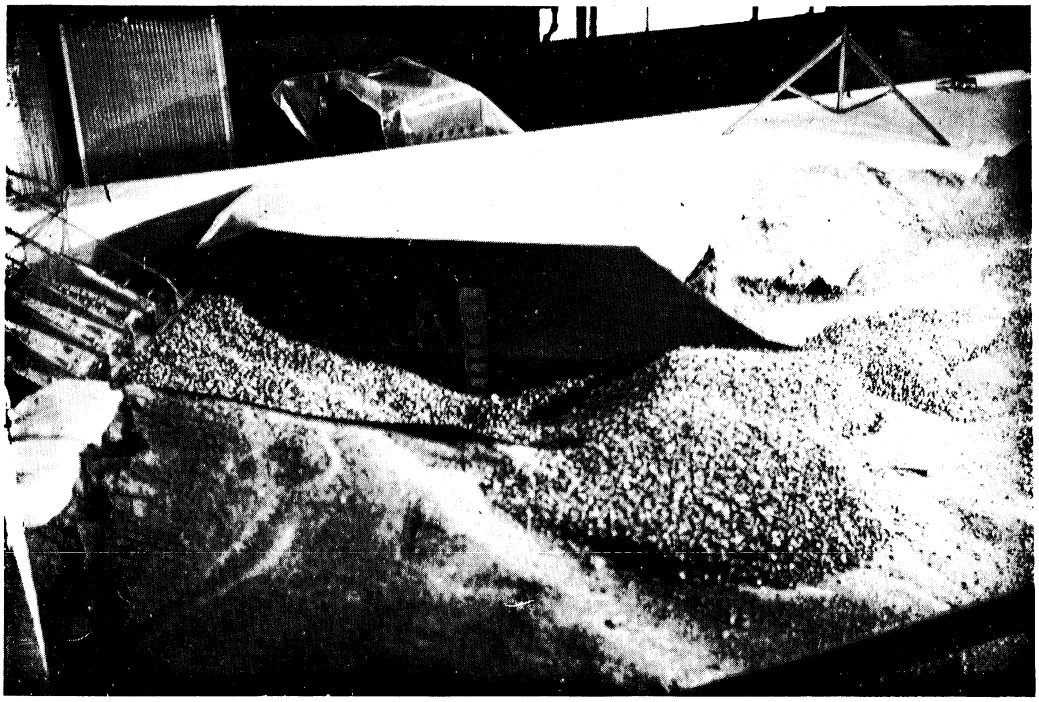

Photo 9 - Scour in Exit Channel and Delta, Q = 3000 cms

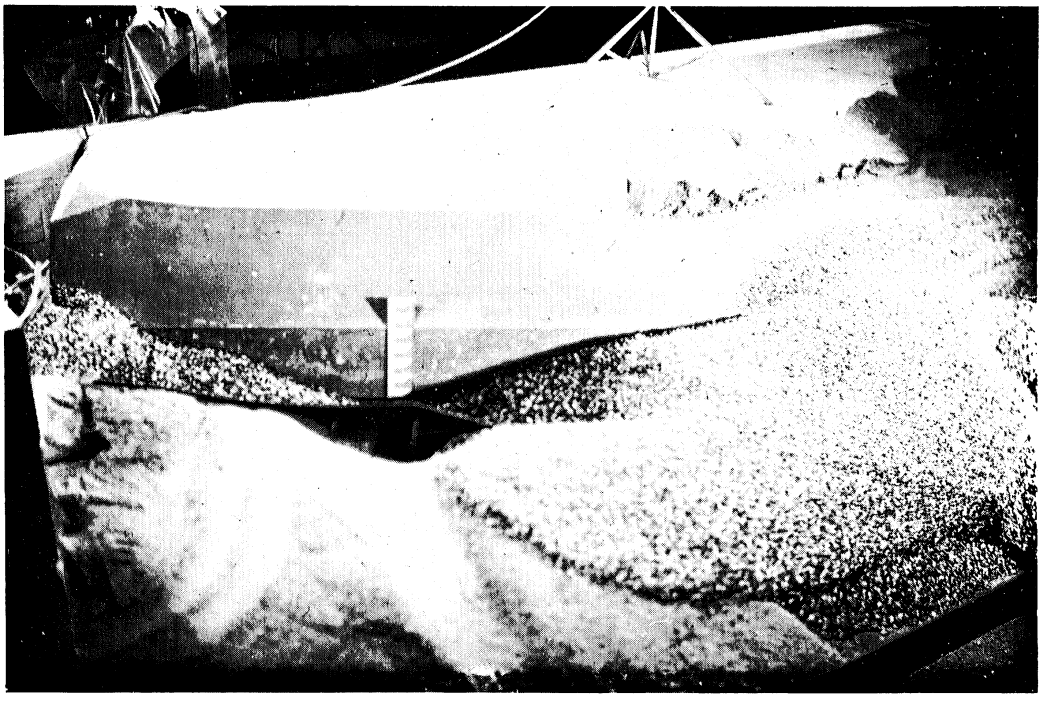

Photo 10 - Scour in Exit Channel and Delta, Q = 5700 cms

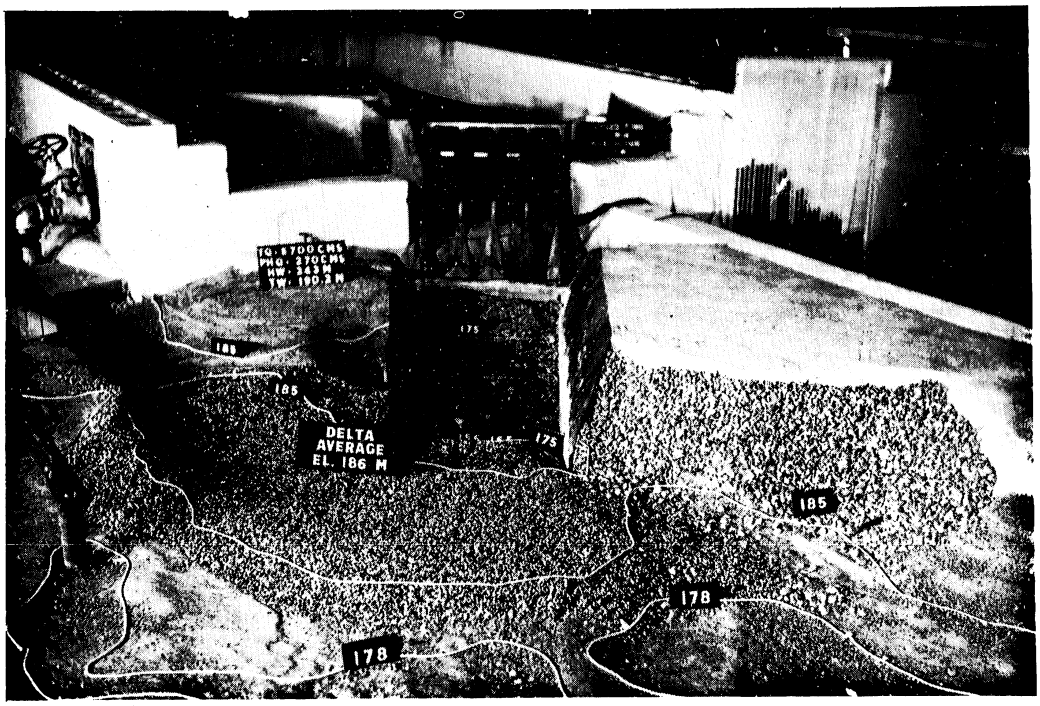

Photo 11 - View of Erosion Pattern after 90 minute run at Q = 5700 cms with Erodible Exit Channel

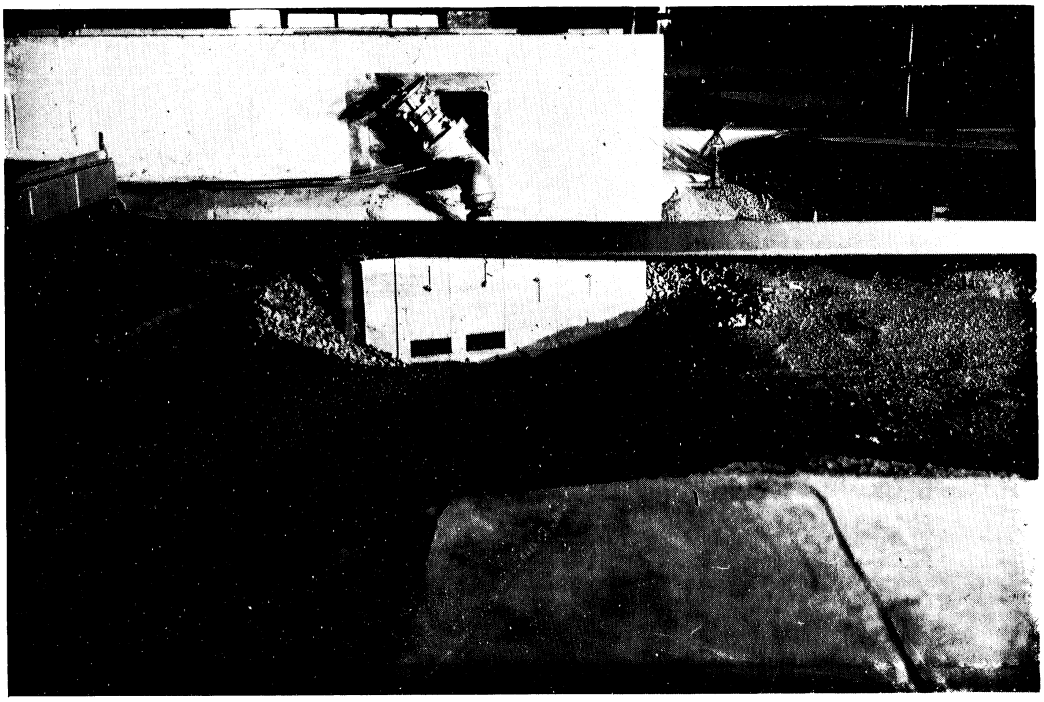

Photo 12 - View of Powerhouse Exit after a run with Q = 5700 cms

Photo 13 - Downstream view of Spillway Flow at Q = 5700 cms with Concrete Exit Channel, very little lateral spreading and energy dissipation

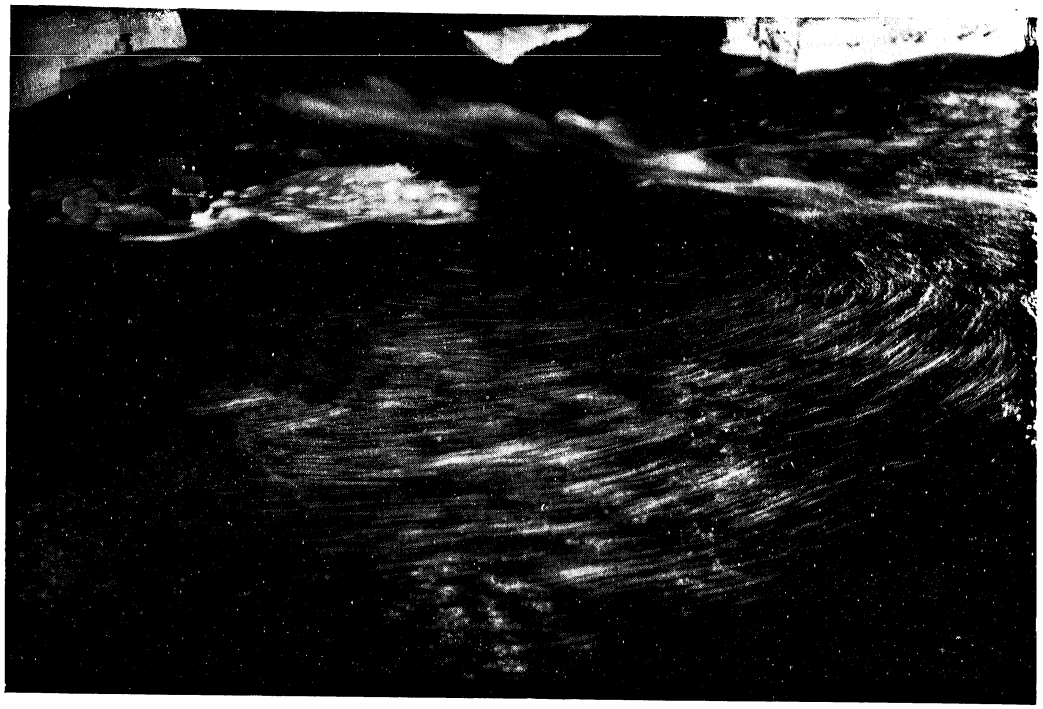

Photo 14 - Large Clockwise-rotating Vortex generated by the Spillway Discharge when Concrete Bed is used for Exit Channel

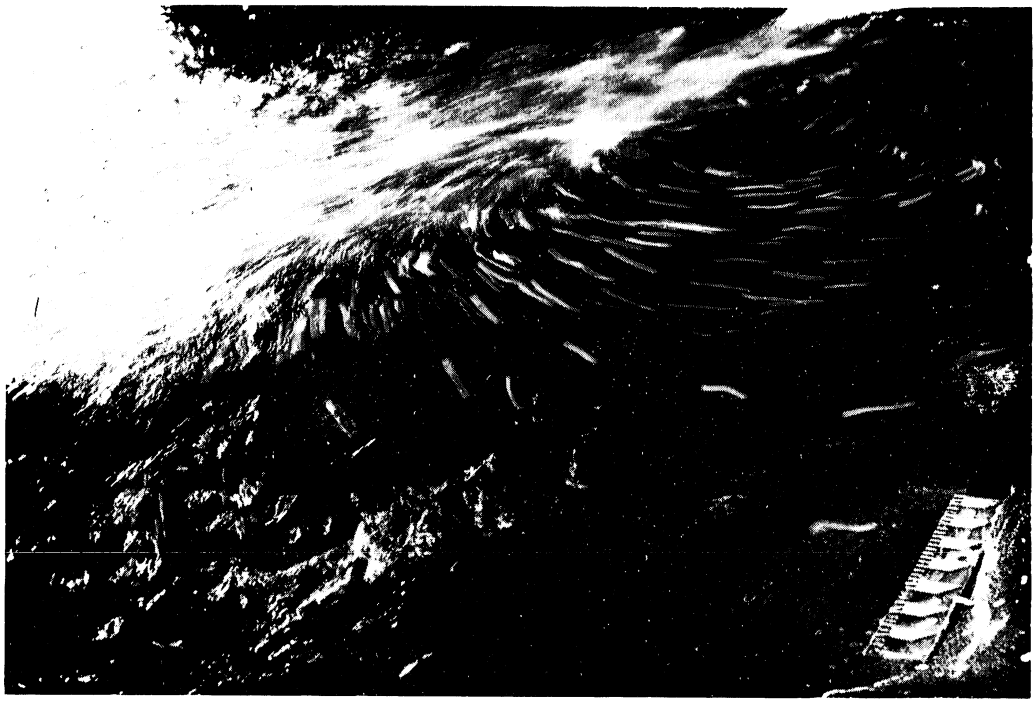

Photo 15 - Very Intensive Counterclockwise-rotating Vortex generated by the Spillway Discharge when Concrete Bed is used for Exit Channel

Photo 16 - Scouring Immediately Downstream of Concrete Exit Channel after 90 minutes of discharge at 5700 cms

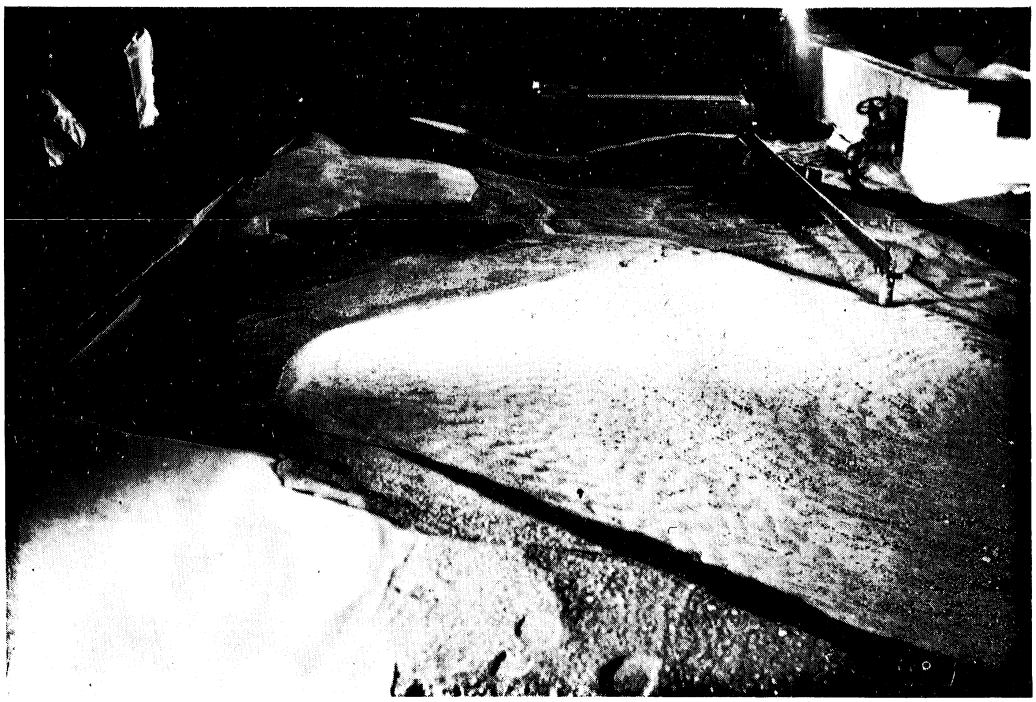

Photo 17 - Sand Bar to the right of the Main Flow formed by the Clockwise-rotating Vortex

APPENDIX

Calibration of Orifice Meter

Near the end of this project a question was raised concerning the accuracy of the calibration curves obtained on this experiment. It was pointed out that the measured spillway discharge for a given headwater elevation measured in the model was substantially greater than the corresponding value computed at the Harza Engineering Company, particularly in the high flow range.

As was explained in the report, the discharge was measured using orifice meters installed in the supply pipes. These orifice meters were calibrated at the beginning of the experiment using a weighing tank. The calibration of the orifice meter in the 12-inch supply pipe was repeated at the end of the test program at the request of Harza Engineering Company. The two sets of data are plotted in Fig. A as curves 1 and 2 for comparison. Although a noticeable difference exists between the two calibration curves, it is apparently too small to account for the difference that Harza Engineering Company has suggested.

The accuracy of the calibration curves can be further demonstrated by the following computation. According to H. Addison*, the discharge through an orifice meter can be written as

$$Q = C_d \, a\sqrt{2gh}\,\sqrt{\frac{1}{1 - m^2}}$$

in which a = Area of the orifice opening

h = Head difference between upstream and downstream of the orifice

m = Ratio of the orifice diameter to the pipe diameter

C_d = Discharge coefficient

For the present case of an 8-inch orifice in a 12-inch pipe, the discharge coefficient is found in the referenced book (Fig. 77, page 138) to be 0.61. Substituting the known constants in the orifice equation, it follows that

$$Q = 1.98\sqrt{h}$$

---

*Hydraulic Measurements, John Wiley and Sons, 1941, pp. 135-138.

in which Q and h are measured in cfs and feet of water, respectively.

The specific gravity of the Blue Merian fluid used for the manometer is 1.75. The orifice equation relating the discharge in cfs and the manometer reading in inches is, then,

$$Q = 0.495\sqrt{h}$$

This equation is plotted as line 3 in Fig. A. Clearly, all three lines are very close to each other, and there is no reason to believe that the calibration might be in substantial error.

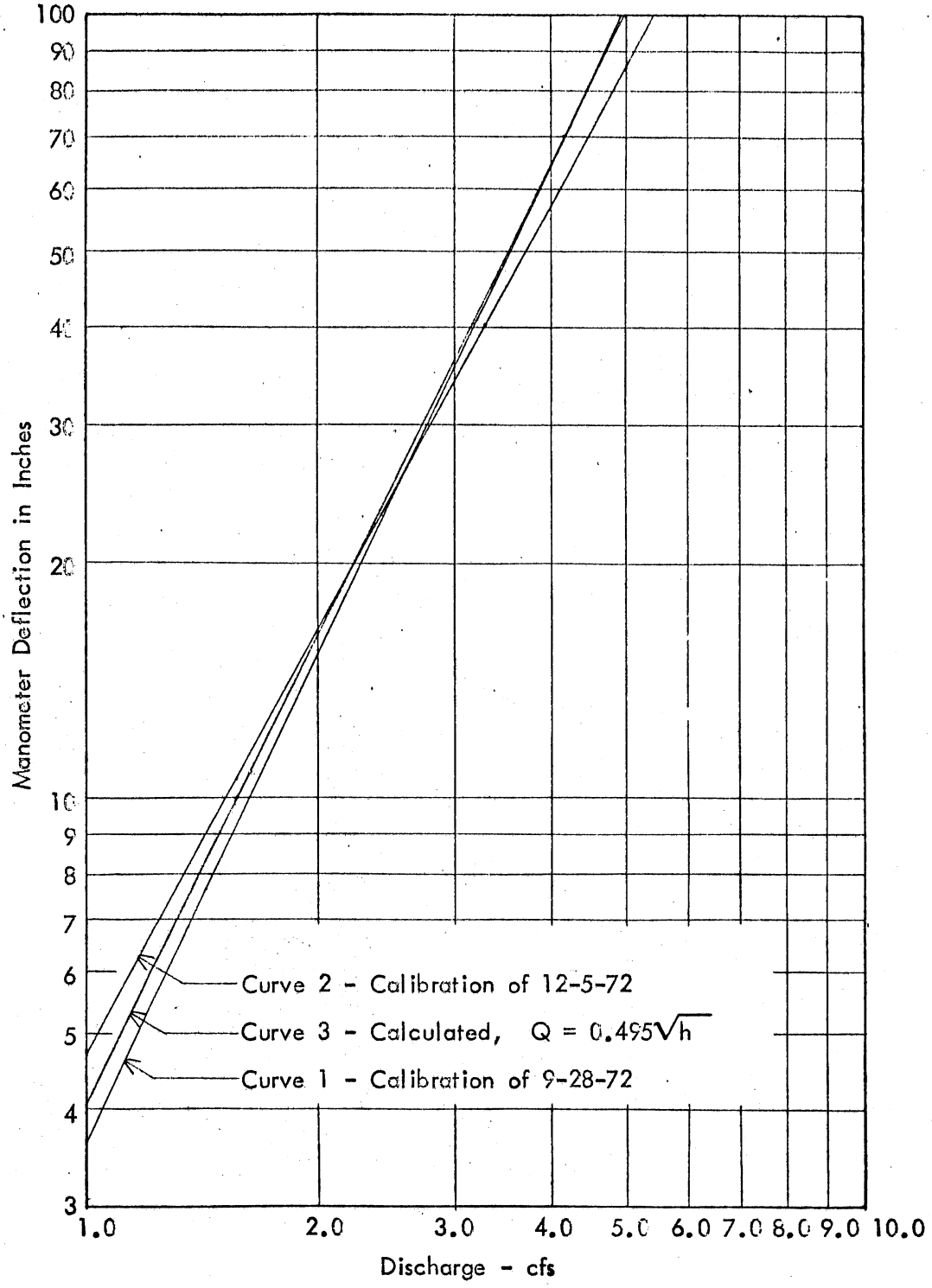

Fig. A - COMPARISON OF CALIBRATION CURVES FOR ORIFICE METER